INVESTIGATIONS OF POLARIZATION SWITCHING OVER BROAD TIME AND FIELD DOMAINS IN VARIOUS FERROELECTRICS

BY

Christelle Jullian

B. S., University of Technology of Compiegne, France, 2002

THESIS

Submitted in partial fulfillment of the requirements for the degree of Master of Science in Materials Science and Engineering in the Graduate College of Virginia Polytechnic Institute and State University.

December the 10th, 2003

Blacksburg, Virginia

Chair: Dr. Dwight Viehland

Committee members: Jiefang Li, Dr. Norman Dowling

Keywords:

Polarization switching; Domain dynamics; Ferroelectrics; Switching mechanisms; Relaxation time; Nucleation.

INVESTIGATIONS OF POLARIZATION SWITCHING OVER BROAD TIME AND FIELD DOMAINS IN VARIOUS FERROELECTRICS

By Christelle Jullian

ABSTRACT

Investigations of polarization switching over broad time and electric field domains, in various modified Pb-based perovskite ferroelectrics, were systematically performed by ferroelectric switching current transient and bipolar drive P-E responses. Studies were performed from E«E_c to E»E_c, where Ec is the coercive field These investigations have shown the presence of broad relaxation time distributions for the switching process, which can extend over several decades in order of magnitude in time, and where the distribution is strongly dependent on the applied electric field.

By performing the study of domain dynamics and polarization switching over extremely broad time domains (10^{-8}<t<10^{2} sec), more complete information has been obtained that allows for development of a better mechanistic understanding. Prior polarization kinetics studies have focused on relatively narrow time ranges, and were fit to the Avarami equation, which contains a single relaxation time. However, our broad band width polarization dynamics and frequency relaxation studies have been fit to multiple stretched exponential functions extending over decades of order of magnitude in the time domain. Stretched exponential functions for domain nuclei formation, and for domain variant growth have been found. For example, $[001]_c$, $[110]_c$, and $[111]_c$ oriented PZN-4.5%PT crystals, nucleation was found to be a volume process (n=3) rather than just a domain wall restricted process. Consequently, nucleation is heterogeneous. And, growth of a domain variant with reversed polarization was found to be a boundary process (n=2), involving diffuse or rough domain walls. We have extended these studies to various types of ferroelectrics including hard, soft and relaxor types.

TABLE OF CONTENTS

LIST OF TABLES

LIST OF FIGURES

CHAPTER 1

INTRODUCTION

1.1. Overview

Ceramic materials are compounds composed of metallic (positive) and nonmetallic ions (negative). Depending on the difference in electronegativity of the constituent atoms, the atomic bonding in ceramics can range from purely ionic (nondirectional) to entirely covalent (directional). Different properties and applications of ceramic materials are therefore implied by variations in the chemical bonding within different crystal structures. During the past fifty years, electronic ceramics have been investigated and improved significantly. Consequently, a new generation of these materials has evolved since World War II. Advancements have provided materials for high-performance applications, and have had a dramatic effect on our way of life. This can especially be seen in the areas of electronics, computers, communications, and aerospace.

The development of ferroelectric (piezoelectric) ceramics also occurred in this time period. Until the 1950's, not much work had been done since the discovery of the piezoelectric direct effect, which dates from the 1880's by the work of the Curie brothers.

1.1.1. What are electronic ceramics?

Generally, they are designated by a chemical compound formula or by a combination of several compounds. Each compound, M_aX_c or $M_aN_bX_c$ is made of one nonmetallic element (X) that forms a stable compound with a metal (M, N) like Oxygen. Many ceramics exhibit a combination of both ionic and covalent bonding. Covalent bonding, although it is stronger, decreases the electrical conductivity dramatically, while, ionic bonding, which is generally weaker, has been shown to exhibit high conductivities. Figure 1-1 illustrates the formation of Mg^{2+} and O^{2-} ions by electron transfer.

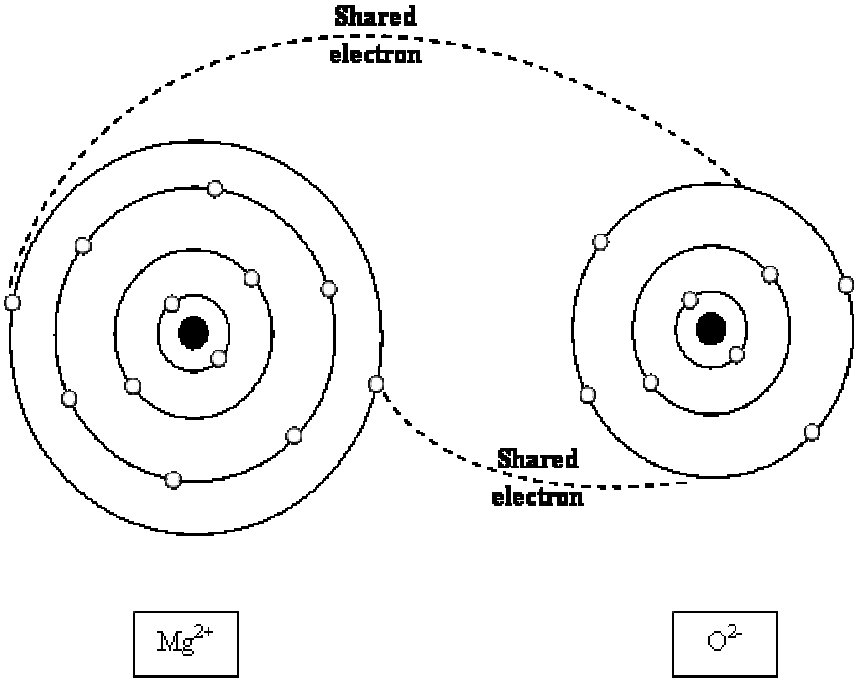

Figure 1-1. Ionic-covalent bonding of MgO due to the sharing of two electrons**.**

1.1.2. Dielectric behavior of electronic ceramics

Dielectric materials are electrically insulative, but still susceptible to polarization. Polarization is the alignment of dipole moments in the presence of an externally applied electric field. There are three sources of polarization: electronic, ionic and orientation, resulting in three types of dipole moments. In the presence of an electric field, dielectric materials exhibit at least one of these polarization types, with the other types being possibly negligible or totally absent.

All dielectric materials induce electronic polarization (Figure 1-2a), which results from the distortion of the negatively charged electron cloud, relative to the positive nucleus of an atom. Only materials with ionic bonds may have ionic polarization, (Figure 1-2b) caused by the relative displacement of cations in one direction and anions in the opposite direction. As a result, net dipole moments are induced on this new structure. Only substances with permanent dipole moments may possess an orientational polarization (Figure 1-2c), which is described as the rotation of the permanent dipole moments into an applied electric field direction. Again, polarization is the alignment of either induced atomic (electronic polarization) or induced molecular (ionic polarization) or permanent (orientation polarization) dipole moments in the direction of an applied electric field. Figure 1-2 shows the three possible sources of polarization depending on the dielectric material, and the way of applying the electric field.

As shown on the figure 1-3a, the electric dipole consist of two charges of equal magnitude but of opposite sign separated by a distance *d*. The electric dipole moment of this configuration defined by the vector *p* directed from $-q$ to $+q$ along the line joining the charge having magnitude *qd*:

$$p = qd \quad ; \tag{1.1}$$

On Figures 1-3(b) and (c), we suppose that this electric dipole is placed in a uniform electric field E. Therefore, the two forces produce a torque T on the dipole, given by:

$$T = dF \sin\theta = dqE \sin\theta = \vec{p} \times \vec{E} \tag{1.2}$$

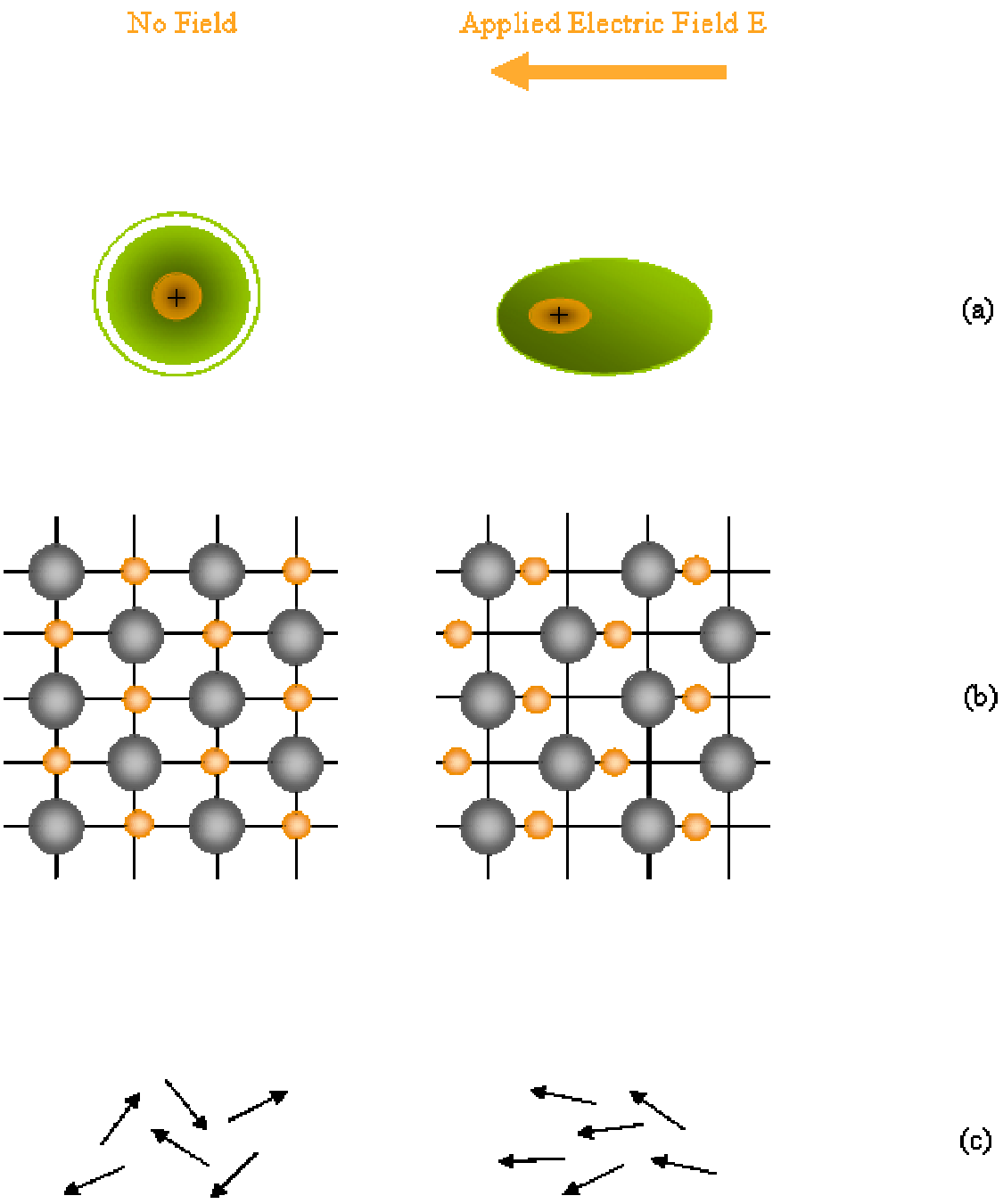

Figure 1-2. The three sources of polarization. (a) Electronic. (b) Ionic. (c) Orientation.

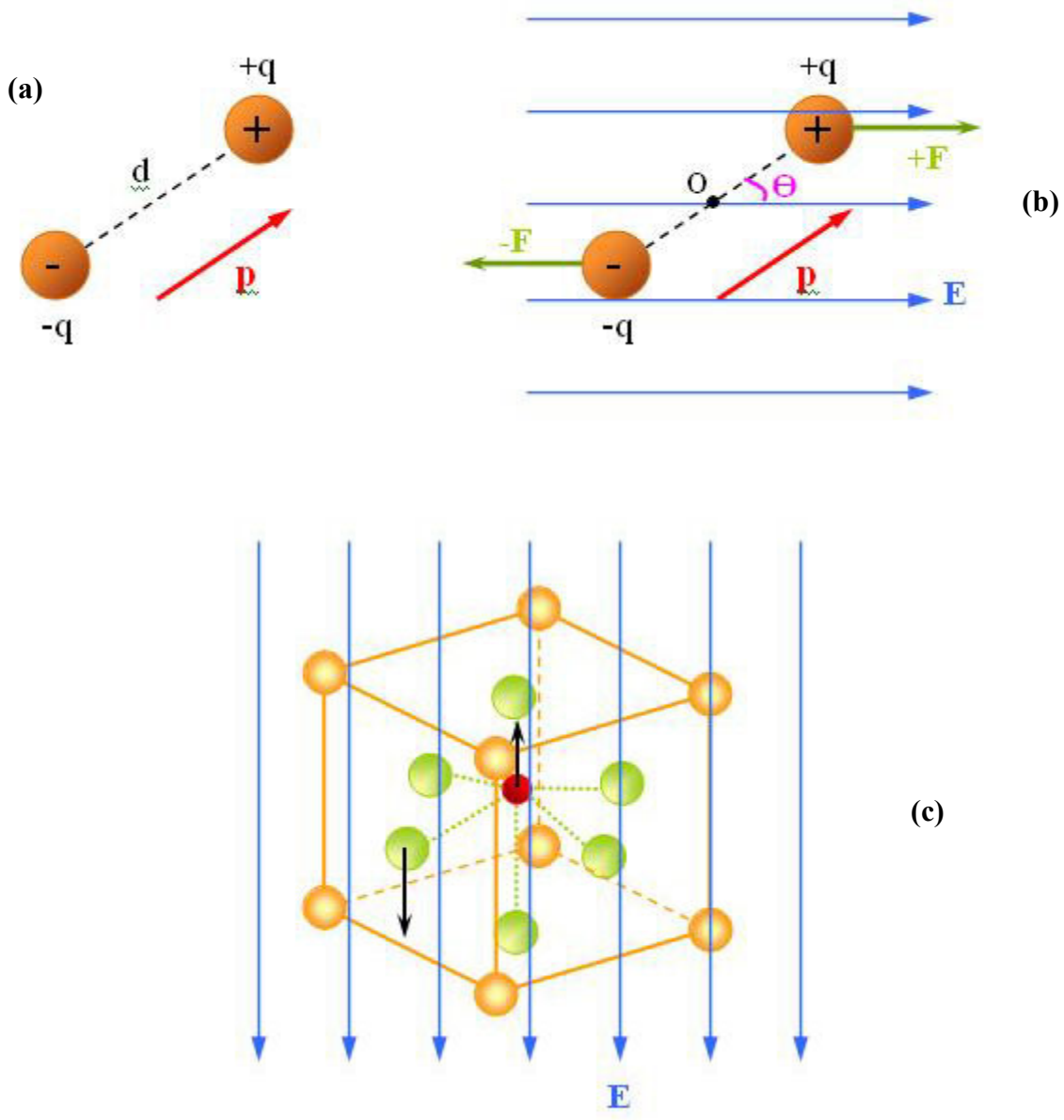

Figure 1-3. Process of dipole alignment with the electric field termed polarization

The polarization P may be thought of as the total dipole moment per unit volume of the dielectric material. Most ceramic materials have dielectric constants within the range of 5 to 10. However, titania (TiO_2) and titanate based ceramics (such as $BaTiO_3$) can exhibit very high dielectric constants, providing great applications as small high power capacitors.

1.2. Piezoelectricity

The piezoelectric effect is the aptitude of certain materials to produce an electric charge, which is proportional to an applied mechanical stress. This is termed the direct piezoelectric effect. By reversing the sign of the stress applied to this material, (from tension to compression) the direction of the electric charge created is reversed as well. The piezoelectric effect is also reversible. When an electric charge is applied, a mechanical strain is created. This property is called the inverse piezoelectric effect.

The piezoelectric effect in a crystal results from the creation of electric dipole moments (polarization) and the establishment of an electric field across the specimen by application of external force. Dipole moments may be induced from three different sources, as explained above. Within the 32 point groups, only 20 are piezoelectric, possessing a unique polar axis in a noncentrosymmetric unit cell. Among these 20 point groups, only 10 have a switchable polar axis. These 10 can display a spontaneous polarization.

The piezoelectric effect is defined as a linear relationship between a mechanical variable (strain *S* or stress *T*), and an electric variable (electric field *E* or electric displacement *D*). On the basis of thermodynamic principles, piezoelectric equations can be derived from the Gibbs free energy *G* of a piezoelectric crystal system in the form,

$$G = U - S_{ij}T_{kl} - D_mE_n - B_mH_n - \sigma\,\Theta, \qquad (1.3)$$

$$(i, j, k, l = 1,2,3,\ldots,6 \text{ and } m, n = 1,2,3).$$

Depending on the boundary conditions externally applied on the specimen, the piezoelectric equations may be written as

$$S_i = s_{ij}^{D}\, T_j + g_{im}\, D_m , \tag{1.4a}$$

$$E_n = - g_{nj} T_j + \beta_{nm}^{T}\, D_m , \tag{1.4b}$$

or,

$$T_j = c_{ji}^{E}\, S_i - e_{jn}\, E_n , \tag{1.5a}$$

$$D_m = e_{mi}\, S_i + \varepsilon_{mn}^{T}\, E_n ; \tag{1.5b}$$

where, g_{nj} and e_{mi} are the direct piezoelectric constants, ε_{mn}^{T} is the permittivity at constant stress, c_{ji} is the elastic stiffness constant, and β_{nm} is the dielectric impermeabilities. The two indices (i, j) of the piezoelectric coefficients respectively stand for the polarization axis direction and for the specimen deformation direction, respectively. Table I shows some of the piezoelectric properties of PZT are listed below.

1.3. Ferroelectricity

Ferroelectric crystals are a subgroup of the piezoelectric materials. Ferroelectrics are distinguishable from piezoelectrics by their aptitude to reverse the spontaneous polarization by the application of an external electric field. This effect, ferroelectricity, was discovered in 1921 by Valasek.

1.3.1. Curie temperature and Phase transitions in ferroelectrics

Ferroelectrics undergo a phase transition corresponding to a change in the crystal structure. This phase transition occurs at a particular temperature and is followed by some electric polarization amplitude and/or orientation modifications. The Curie point $T_{c,}$ is the temperature from which the ferroelectric crystal undergoes a structural phase transition, from a paraelectric phase at $T>T_c$ (the spontaneous polarization is vanished) to a ferroelectric one at $T<T_c$ (with a spontaneous polarization). The dielectric constant reaches its maximum value at the Curie point. Above T_c, the crystal is paraelectric and

Composition	ε_r	$s_{\alpha\beta}$	di_β	ki_β
Ferroelectric $Pb(Zr,Ti)O_3$	200-5000	10-20	100-1000	0.3-0.8

Table I. Some of the piezoelectric properties of PZT.

does not exhibit any ferroelectricity and the dielectric constant follows the Curie law,

$$\varepsilon_r = \frac{C}{T - T_0} = \frac{\varepsilon}{\varepsilon_0}, \tag{1.6}$$

where C is the Curie constant, T is the absolute temperature (K), T_0 is the Curie-Weiss temperature (K), and ε_0 is the permittivity of free space.

Below T_c, the crystal exhibits ferroelectricity. The ferroelectric structure is created by a distortion of the paraelectric structure. As a result, the ferroelectric phase always has a lower symmetry than the paraelectric one. At $T<T_c$, the ions move from their equilibrium position (in the paraelectric phase) to create a spontaneous polarization. When a crystal is cooled down below T_c, the paraelectric-ferroelectric phase transition may be of two types: displacive or order-disorder. Ferroelectrics with a perovskite type structure exhibit a phase transition of the first type, i.e. displacive. Sequential structural phase transitions may occur in addition to the paraelectric to ferroelectric one. For instance, $BaTiO_3$ has three ferroelectric phases below 120˚C (T_c) and their phase transition temperatures are 0˚C and -80˚C. Figure 1-4 represents the atomic displacement occurring at T_c, when the paraelectric-ferroelectric phase transition happens.

1.3.2. Ferroelectric domains

A ferroelectric material is spatially divided into multiple regions with a uniform polarization. Such regions are called ferroelectric domains. In a polydomain condition, the crystal is globally nonpolar, possessing a spherical symmetry of ααm. The interface between two domains is called a domain wall. A domain wall tends to decrease its width, in order to minimize the elastic energy generated by the strain near the wall. Consequently, domain walls tend to be very thin and generally on the scale of a few lattice cells.

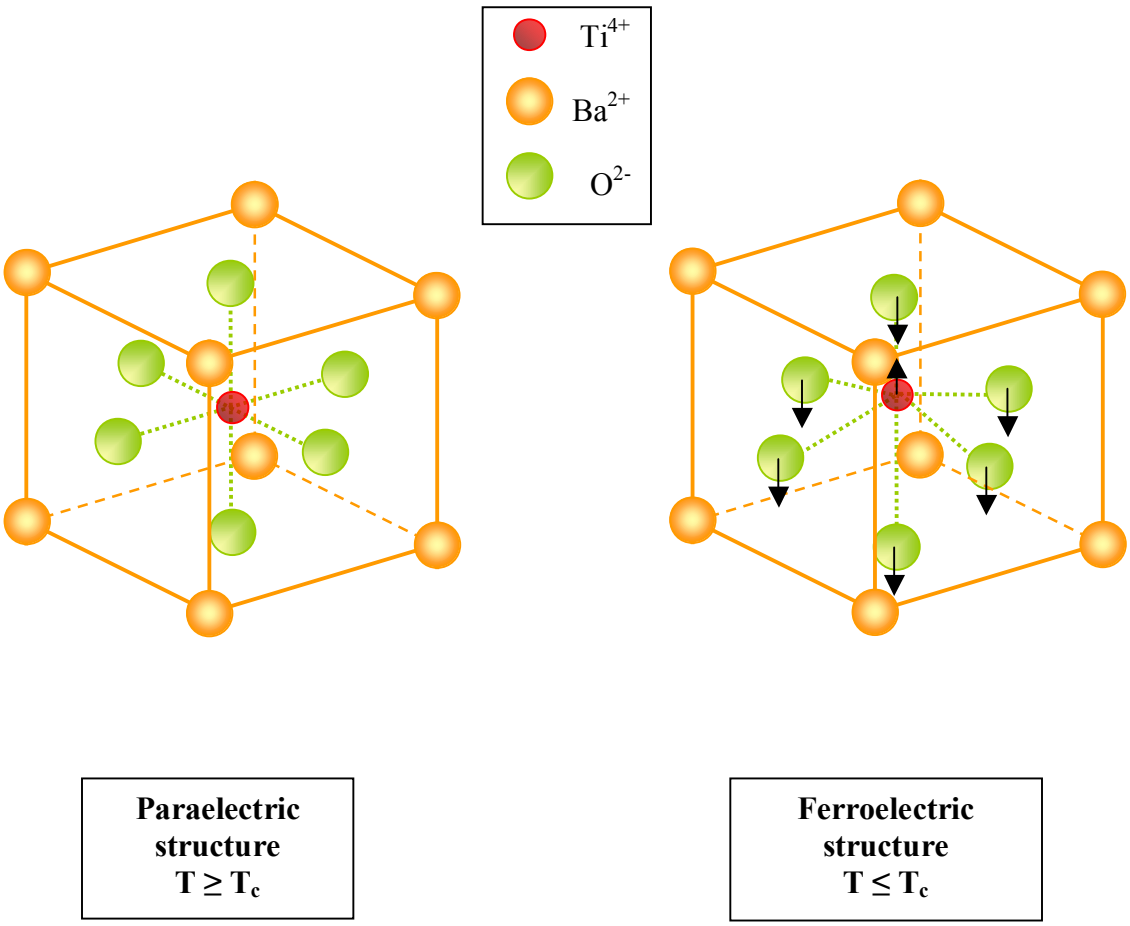

Figure 1-4. Paraelectric-ferroelectric phase transition in $BaTiO_3$ occurring at 120˚C (T_c)

Due to elastic compatibility, the angles between the domains are well defined, and determined by the symmetry of the ferroelectric phase. For example, in a tetragonal ferroelectric phase, the angles are either 90˚ or 180˚, whereas in a rhombohedral phase, they can be 71˚, 109˚ or 180˚. Generally, 180˚ domains can be reversed with only minimal structural strains. However, switching of 71˚, 90˚ or 109˚ domains require significantly larger deformations.

1.3.3. Polarization reversal process in ferroelectrics

When an external electric field is applied to a ferroelectric specimen, the domains more closely align to the external field direction grow to the detriment of the others. This is called the polarization process. Anisotropy in the ferroelectric crystal is large. The variety of both domain patterns and the domain wall types depends on the number of possible equivalent polarization orientations.

Figure 1-5 illustrates the polarization process occurring in a ferroelectric specimen when an electric field is applied. Starting with 90˚ and 180˚ domain patterns, the permanent dipole moments begin to rotate towards the direction of an externally applied electric field. When the electric field is removed, some dipole moments rotate back, but not completely, resulting in a remanent polarization.

1.3.4. The hysteresis loop of a ferroelectric

An important characteristic of a ferroelectric is the hysteresis loop (Figure 1-6). The polarization P is a double-valued function of the externally applied electric field E. If a small electric field is first applied, only a linear relationship between P and E (segment OA) exists because domains stay in their initial configuration. As the electric field strength increases, the domains, whose the polarization direction is opposite to the field will be switched. Consequently, the polarization increases significantly (segment AB) with increasing E until all of the domains are aligned in the field direction. This state is called the state of saturation (i.e., linear segment BC). The value of the spontaneous

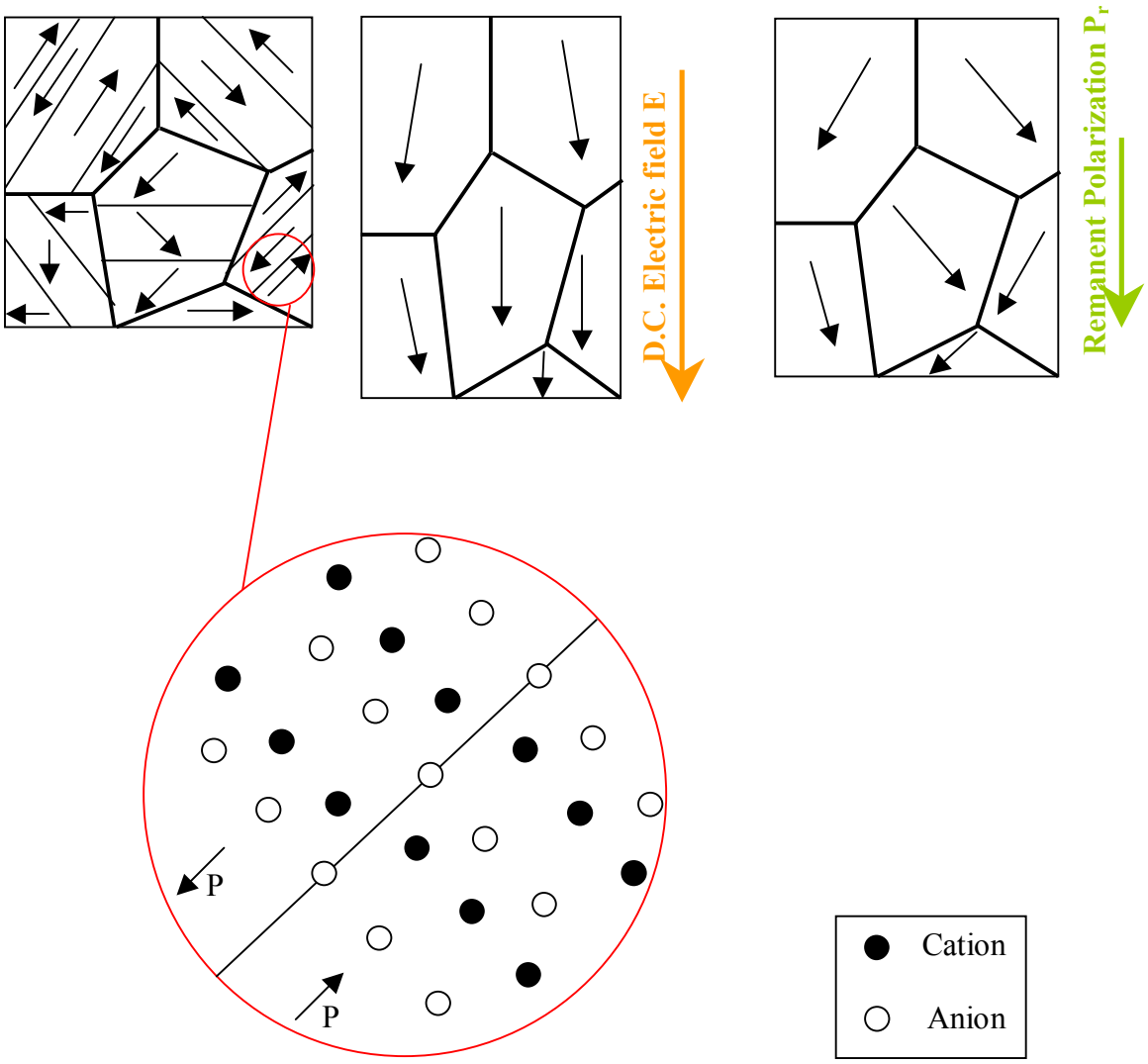

Figure 1-5. Polarization process planar representation

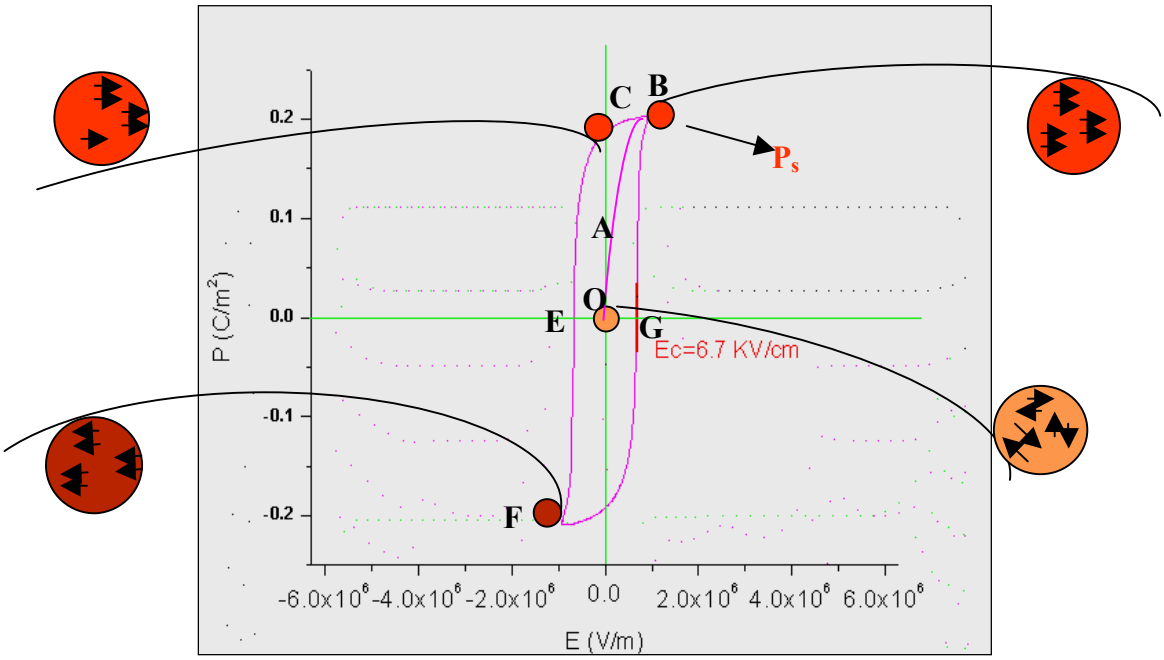

Figure 1-6. Hysteresis loop of a ferroelectric ceramic

polarization P_s is the extrapolation of the segment BC of the hysteresis loop back to the polarization axis. Theoretically, this state of polarization saturation should correspond to a single domain state of the crystal. When the field is decreased to zero, the polarization does not return back to zero. Rather, the domains remain aligned, and the crystal exhibit a remanent polarization P_r. The strength of the field necessary to reduce the polarization to zero is called the coercive field E_c (point E). Further increase of the field in the opposite direction will cause a complete alignment of the dipole domains in this opposite direction (point F). Finally, by reversing the field once again, the process can be repeated.

1.4. Perovskite type ferroelectric

The general chemical formula of the perovskite structure is ABO_3 where O is oxygen. A represents a cation with a larger radius for which the valence may vary from +1 to +3. B is a cation with a smaller radius for which the valence may vary from +3 to +6. A perovskite structure can be thought as a BO_6 octahedron network. Figure 1-7 shows a cubic cell of a perovskite type structure.

1.4.1. The Pb (Zr, Ti) O_3 crystalline solution

Both $PbTiO_3$ and $PbZrO_3$ are perovskite type crystals. Table II summarizes some of the characteristics of both materials. Below their respective T_c, Curie temperatures, $PbTiO_3$ is in a tetragonal ferroelectric phase, where the dipole moment in neighboring unit cells are aligned parallel; whereas $PbZrO_3$ is in an orthorhombic antiferroelectric phase, where the dipole moments in neighboring cells are aligned antiparallel. The Ti^{4+} ions in $PbTiO_3$ can be partially substituted by Zr^{4+} with a molar ratio X to form a binary system (solid solution) with the following chemical formula $Pb(Zr_x\ Ti_{1-x})0_3$. This solid solution is called lead zirconate titanate (PZT). It also belongs to the perovskite-type ferroelectrics. In this solution, Zr^{4+} and Ti^{4+} occupancy on the B-site cation positions is random.

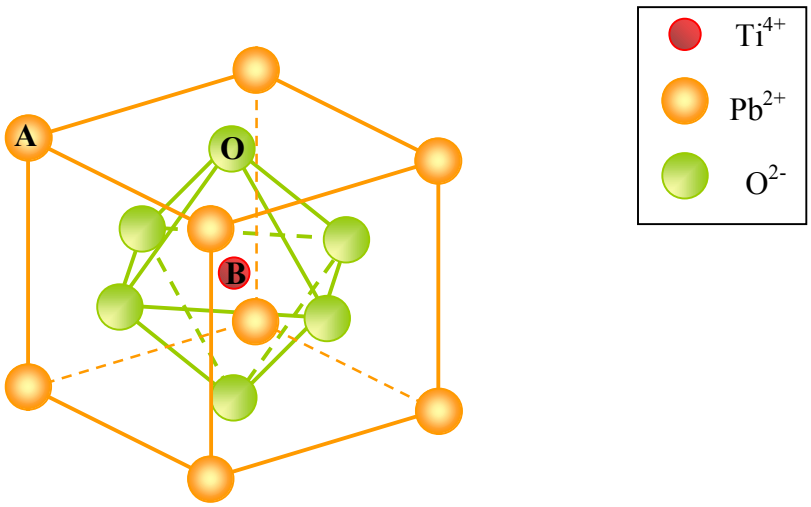

Figure 1-7. Cubic perovskite-type structure of $PbTiO_3$

Compound	Symmetry at room temperature	Lattice parameters a=b (α)	Transition temperature (˚C) to cubic paraelectric phase
$PbTiO_3$	Tetragonal 4mm	3.905	490
$PbZrO_3$	Orthorhombic	4.159 (90˚)	232

Table II. Summarize of some of the characteristics of $PbTiO_3$ and $PbZrO_3$

Figure 1-8 shows the phase diagram of the PZT pseudo-binary system, where T_c is the boundary between the cubic paraelectric phase and the various possible ferroelectric/antiferroelectric phases. A morphotropic phase boundary (MPB) divides the ferroelectric region in two parts, which are the rhombohedral (Zr-rich side) and the tetragonal (Ti-rich side). The MPB is located near X~50%. The width of the MPB depends on processing, and may also be modified by substituents.

The compositions close to or at the MPB are quite interesting. This is because they have high dielectric and piezoelectric properties. In the tetragonal phase, there are six equivalent (100) polarization directions; whereas in the rhombohedral phase, there are eight equivalent (111) variants. Within the MPB region, the 6 domain states of the tetragonal coexist with the 8 domain states of the rhombohedral. This results in 14 possible directions for the spontaneous polarization. Consequently, the piezoelectric coefficient, dielectric permitivity and remanent polarization of PZT ceramics reach a maximum for compositions close to the MPB region.

1.4.2. Modified PZT piezoelectric ceramics

PZT ceramics are normally modified by adding substituents, which optimizes their utility for particular applications. Substituents are known to result in significant changes in domain structures and electromechanical properties, because they create various types of defects in the crystal structure. Defects may result in, (i) an increased coercive field E_c if they are randomly distributed, or (ii) an internal biasing of the hysteresis loop, if the defect dipoles have the same orientation. There are three general types of substituents. These are (i) isovalent, which only slightly affect properties, (ii) lower valent that tend in perovskites to be charged compensate by oxygen vacancies, (iii) higer valent ones that tend to be compensated by Pb-vacencies. Lower valent substituents tend to make PZT "harder", whereas, higher valent ones make it 'softer'.

Table III summarizes the general characteristics of soft, relaxor and hard ferroelectric ceramics compare to PZT.

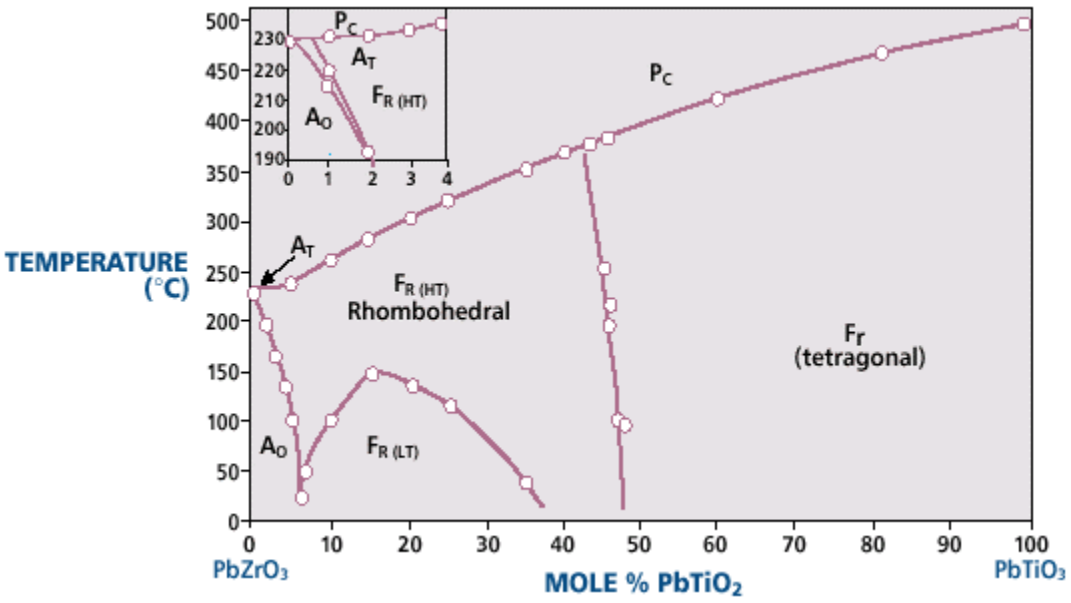

Figure 1-8. PbTiO3-PbZrO3 solid solution phase diagram.

Soft	Relaxor	Hard
Dielectric constant ε ↑	Dielectric constant ε ↑↑	Dielectric constant ε ↓
Dielectric loss factor ↑		Dielectric loss factors ↓
Hysteretis loss ↑	Very small hysteretis loss	Hysteretis loss ↑↑
Elastic compliance ↑		Elastic compliance ↓
Piezoelectric planar coefficients ↑	Null Piezoelectric planar coefficients	Piezoelectric planar coefficients ↓
Electrical resistivities ↑		
Mechanical loss factor ↑		
Coercive field E_c ↓	Coercive field E_c ↓↓	Coercive field E_c ↑
The Curie point T_c ↓	The Curie point T_c ↓↓ Frequency dependence of T_c	The Curie point T_c ↑
The remanent polarization P_r ↓	No remanent polarization P_r	The remanent polarization P_r ↑
The remanent strain ↓	No remanent strain	The remanent strain ↑

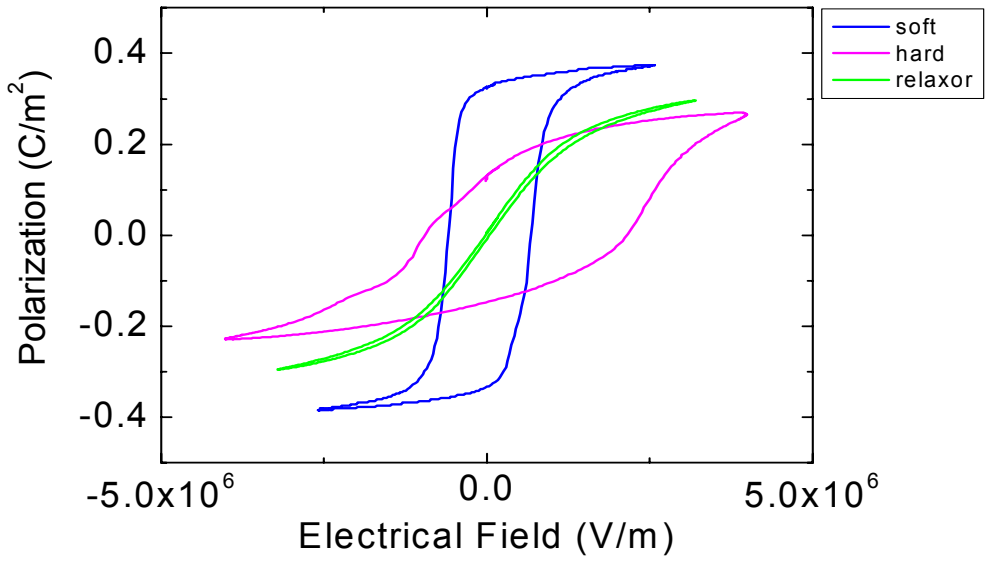

Table III. General characteristics of soft, relaxor and hard ferroelectrics.

1.4.2. (a) Soft PZTs

Soft PZT behavior can be induced by higher valent substituents in PZT. For example, La^{3+} or Nd^{3+} can be substituted into the A-site, whereas Nb^{5+} or Sb^{5+} are some possible substituents for the B-site. Soft ferroelectrics have higher dielectric constants, higher dielectric and mechanical loss factors, higher elastic compliances, and higher piezoelectric coefficients. However, they have lower coercive fields E_c, lower Curie temperatures T_c, lower remanent polarizations P_r, and lower remanent strain. Soft ferroelectrics also de-pole relatively easily. Amongst the higher valent modified PZTs, $(Pb_{1-3/2y}, La_y)(Zr_{1-x}\ Ti_x)O_3$ crystal or PLZT is a common crystalline solution.

1.4.2. (b) Hard PZTs

Hard ferroelectric characteristics can be induced by lower valent substituents. For exemple, the A-site position can be substituted with K^+ or Na^+; whereas Fe^{2+} or Mn^{2+} can be substituted on the B-site. Hard ferroelectrics have higher coercive field E_c, and higher dielectric losses; but have lower dielectric and piezoelectric constants, and lower electromechanical coupling coefficients. Domain boundary pinning effects have been investigated, and are believed to be the origin of "hard" ferroelectric behavior. Interactions between defects and domain boundaries are believed to stabilize the microstructure and to make domain wall motion difficult. For example, increasing the K content in PKZT results in changes in microstructure-property relationship.

- Rapid decrease of the domain size,
- Apparition of irregular wavy domain patterns. Polar cluster or nano-domains are infrequently found.

1.4.3. <u>$Pb(Mg_{1/3}, Nb_{2/3})O_3$-$PbTiO_3$ and other relaxor ferroelectrics</u>

Relaxor ferroelectric behavior is found in PMN-PT, $Pb(Mg_{1/3},Nb_{2/3})O_3$. Frequency dependence of the Curie Temperature T_c characterizes ferroelectric relaxors.

T_c is the temperature at which the dielectric constant is maximal. Relaxors are characterized by a very slim hysteresis loop (P-E), small E_c, no remanent polarization, higher dielectric constants than soft ferroelectrics, and null piezoelectric constants. Higher valent modifications of high concentration, for instance PLZT 10/65/35, have been investigated. The magnitude of the quenched random field generated by charged compositional fluctuations is insufficient to overcome the long-range ferroelectric interactions. Under electric field, polar cluster are nucleated in the vicinity of the quenched random fields. For fields smaller than E_c, this results in a hierarchy of domain features with subdomain irregularities of a reversed polarization within normal micron-size domains. However, for fields greater than E_c, twin boundary elimination/motion occurs, resulting in complete switching of the remanent polarization. When the electric field is removed, the crystal comes back to its original polarized state. Microstructure-property relationship of Relaxor has been widely investigated **[1]**.

1.4.4. Poled oriented PMN-xPT and PZN-xPT single crystals

Solid solutions PMN-PT and PZN-PT have been widely investigated in the last decade as very promising crystals. PT is a ferroelectric with a tetragonal symmetry (4mm) at room temperature, while PMN and PZN are relaxor ferroelectrics with rhombohedral symmetry (3m). The PZN-PT crystalline solution exhibits a MPB in the vicinity of 8-10%PT volume content, whereas the PMN-PT Morphotropic Phase Boundary is around 30-35%PT. Both PZN-PT and PMN-PT have shown large piezoelectric and electromechanical coupling properties, a hysteresis free strain versus electric field behavior, and relatively high Curie Temperature. It is believed that such superior characteristics arise from a domain engineered crystal structure.

Oriented PZN-PT single crystals were first found to exhibit giant piezoelectric and electromechamical coupling coefficients (respectively d_{33}~1800 pC/N and k_{33}~0.94) by Kuwata et al. **[2]**. Similar high values have also been measured for PMN-PT. Maximum property coefficients are found in the vicinity of the MPB between rhombohedral (FE_r) and tetragonal (FE_t) ferroelectric phases. The enormous responses

have been attributed to the presence of intermediate monoclinic ferroelectric phases (FE_M) **[3-7]**. Several monoclinic phases have been found, including (i) a FE_{Mc} with the polarization constrained to the $(011)_c$ plane; (ii) a FE_{Ma} with the polarization constrained to $(010)_c$; and (iii) a FE_{Mb} with the polarization constrained to $(100)_c$, which has been found only for $(110)_c$ oriented crystals under field. Polarization rotation instabilities under field within FE_M phases **[8-9]** are known, where rotation occurs against a very small anisotropy, and thus the hysteresis is negligible. For a field applied along $(001)_c$, the rotational pathway has been predicted to be $FE_{Ma} \rightarrow FE_{Mc} \rightarrow FE_t$. Investigations of the induced polarization (P) have shown significant differences depending upon whether the crystals are driven under unipolar or bipolar electric field (E) **[10-11]**. For both $(001)_c$ and $(110)_c$ oriented crystals, unipolar drive results in anhysteretic P-E responses, whereas bipolar drive results in significant hysteresis. Clearly, domains are important in polarization switching under bipolar drive, however most investigations have focused on unipolar operation.

The electromechanical properties of <001> oriented PMN-30%PT single crystals have been investigated by P-E and ε-E methods under uniaxial stress **[11].** The results demonstrate that <001> oriented single crystals have a smaller hysteretic loss than the corresponding polycrystalline composition, due to the off-axis nature of polarization vectors within individual grains of polycrystalline, with respect to that of the applied electric field. Also, for both crystal and polycrystalline specimens, a partial depoling occurs under stress, which causes the zero-point strain to be shifted.

Scanning Force Microscopy of domain structures in unpoled and poled PZN-8%PT and PMN-29%PT single crystals, have been performed using <001> and <110> oriented plates **[12]**. The SFM images show a complicated fingerprint pattern of antiparallel polarization domains for the unpoled PZN-8%PT and PMN-29%PT. Antiparllel domain wall are not sharp compared to classical ferroelectrics like $BaTiO_3$. The antiparallel region width range from 0.1μm to 10 μm, and it is smaller in PMN-29%PT than in PZN-8%PT crystals. Macroscopically (optical microscope), long ferroelastic domains are also observed. <001> and <110> poled crystals of PMN-29%PT

and PZN-8%PT do not show a typical ferroelastic domain pattern, but the antiparallel structure again.

1.5. Prior studies of polarization dynamics

In normal ferroelectrics, polarization dynamics have been extensively investigated in normal ferroelectric materials by measuring current transients in response to square wave electrical pulses of reverse bias. The kinetics have been modeled using a modified Avarami equation, given as

$$J(t) = (2P_o n/\tau)\,(t/\tau)^{n-1}\exp[-(t/\tau)^n] \qquad (1.7a)$$

or,
$$P(t) = P_o \exp[-(t/\tau)^n]; \qquad (1.7b)$$

where $J(t)$ is the current density as a function of time, $P(t)$ is the polarization as a function of time, P_o is the induced polarization, n is the dimensionality of the switching process, τ is the characteristic relaxation time, and t is the elapsed time since application of electric field.

However, limiting the study of domain dynamics and polarization switching has been that current transient investigations have been performed over relatively narrow time (t) and electric field (E) ranges **[13-20]** even though the current response is known to be logarithmic in time **[18,21-24].** Analysis of the dynamics in the time domain of $10^{-8}<t<10^{-6}$ sec has provided incomplete information, upon which to develop a mechanistic understanding. Various investigations have used equation 1.7b Early investigations by Merz **[13]** revealed a model for polarization reversal where 2-D nucleation of reversed clusters occurs on existing 180° domain walls and where 1-D growth of reversed step-like domains occurs perpendicular to the direction of E. In this model, nucleation is confined to the domain wall, and during domain growth the twin wall is restricted to be coherent, as illustrated in Figure I-9. It is known that in finite-size systems that the Merz model is in applicable **[25],** and has been extended by Scott et al.

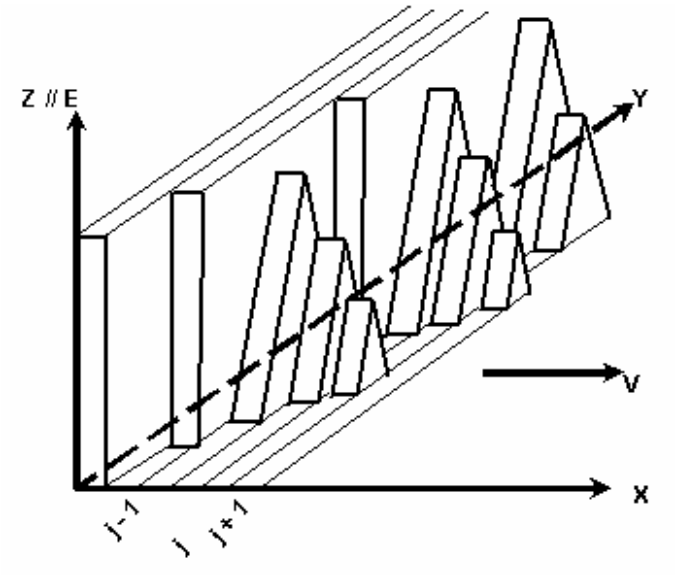

Figure 1-9. Merz model of nucleation and growth

[26] to account for spatially limited conditions.

Analysis of data has resulted in important differences to what should be expected using 1.7. First, analysis has shown fractal exponents, whereas strict use of 1.7 requires integer values. Recent analysis by Shur et al. [16] has attempted to resolve this difference by allowing n to change between integer values. This change was attributed to a geometric catastrophe, conjectured to result from domain impingement. Second, analysis has revealed that nucleation and growth is at most a 2-D process, generally with an average dimensionality constant of ~1.5. However, both homogeneous and heterogeneous nucleation and growth is a volume (i.e., 3-D) process. Finally, analysis of ferroelectric switching currents with 1.7 has tended to under predict the current at longer times of $t>4t_{max}$, where t_{max} is the time of the current maximum. This results in a skewing of the current transient peaks to longer times in the time domain of $10^{-8}<t<10^{-6}$ sec **[16,18-20].**

In ferroelectric domain theory, the importance of defects has been considered [27] as preferred nucleation sites. Prior investigations [24] have shown a stage in polarization switching that depends on logarithimic time. But, not until recent studies by Scott [26] and by Viehland et al. [22,23] have defects been considered to play a vital role in polarization dynamics.

Recently, in PMN-x%PT, (that exhibits the same high piezoelectric properties as PZN-x%PT) skewing has been understood by stretched exponential functions that include the effect of random fields, which broaden nucleation and growth events in the time domain [22]. Also, recent P-E studies have revealed pronounced dispersion in the frequency domain of $10^{-2}<f<10^{2}$ Hz **[23].** The polarization dynamics and frequency relaxation of PMN-x%PT have been analyzed using stretched exponential functions [28-30] which have terms in $[\ln(t/\tau)]^n$, given as

$$P(t) = \sum_{i=1}^{k} P_{o_i} \exp\left\{ - a_i \left[\ln\left(t / \tau_i \right)^{n_i} \right] \right\}, \qquad (1.8)$$

where $P(t)$ is the time dependence of the polarization, P_{oi} is the nucleated polarization in the i^{th} switching time domain, k is the number of switching time domains considered to calculate the total polarization, n_i is the dimension of the nucleation in the i^{th} switching time domain, τ_i is the average relaxation time of the i^{th} switching time domain, and a is an exponential factor. This equation has similarities to the Avarami relationship given in (1.7b), where terms in $(t/\tau)^n$ have been replaced by ones in $[\ln(t/\tau)]^n$. Substitution with $\ln(t/\tau)$ will result in a significant extension to longer times of the long-time tail of the nucleation curve, relative to a similar relationship in terms of (t/τ). Also, equation (1.8) predicts that ln(P) depends on ln(t), which will result in significantly stronger broadening in the time domain than a simple dependence of P on ln(t).

Stretched exponential behavior is well known in disordered systems **[31-33]**. It is a form of hierarchial relaxation. In random-field theory, nucleation of domain boundaries under field occurs in the vicinity of quenched defects that are conjugate to the applied ordering field. Consequently, domain walls become diffuse and polar nanoregions (PNR) can be created. Many modified perovskite ferroelectrics are known to contain significant quenched disorder, such as PMN-x%PT and PZN-x%PT **[34-37].** Interestingly, electron microscopy studies of poled soft ferroelectrics ceramics by Tan et. al. **[38]** have previously shown domain breakdown with increasing AC electric field, which is consistent with polarization switching through a relaxor state. After weak field drive, normal micro-sized domains were found. However, after modest AC drive (1-3 kV/cm), specimens of the same composition were found to consist of PNRs. Correspondingly, dielectric constant measurements under weak field drive exhibited normal ferroelectric behavior, where as that under 1-3 kV/cm exhibited relaxor behavior.

CHAPTER 2

PURPOSE OF RESEARCH

The dynamics of polarization switching have been investigated over extremely broad time ($10^{-8}<t<10^{2}$ sec) and field ranges ($E\leq\sim4E_C$) for various modified Pb-based perovskite ferroelectrics. Defects and substituents are known to significantly influence the electromechanical properties of ferroelectrics. The purpose of this thesis is to study domain dynamics for various types of ferroelectrics, commonly called "soft", "hard" and "relaxor". This is done to provide information to develop a mechanistic understanding of polarization domain switching. This thesis will demonstrate that these three families of materials may be characterized by different trends in the current transient response, depending upon the existence of broad relaxation time distributions, and upon which time domain they occur ($10^{-8}<t>10^{2}$ seconds).

In Chapter 4, broad relaxation time distributions for polarization switching were observed over broad field ranges of ($0<E\leq3E_c$) for various modified Pb-based perovskite polycrystalline ferroelectrics. This relaxation time can extend over decade(s) in orders of magnitude in time, and is extremely dependent on E. Similar results were found for three "soft" ferroelectrics compositions, PLZT 7/65/35, PMN-30%PT, and a commercial "soft" PZT.

Chapter 5 deals with polarization switching dynamics over broad time and field ranges for oriented PZN-4.5%PT single crystals. The polarization transients have been fit to stretched exponential functions in time, which are typical of highly disordered systems. At relatively small fields, $E\ll E_c$, nucleation is found to be heterogeneous (n=3), whereas growth of new domains is a boundary process (n=2). Analysis of the data has shown important differences to what is expected using the commonly modified Avarami equation. At higher fields of $E\gg E_c$, polarization switching was found to occur by a mechanism similar to conventional ferroelectric domain nucleation and growth.

In Chapter 6, polarization switching in “hard”, “soft”, and “relaxor” Pb-based perovskite polycrystalline ferroelectrics, has been comparatively studied, over broad time and field ranges. The results demonstrate important differences in the polarization switching mechanisms for these various ferroelectrics. It was shown that domain growth is not significant for “hard” PZT, whereas “soft” PZT exhibits extremely broad nucleation and growth events. And, in relaxor ferroelectrics, polarization reversal occurs entirely by nucleation.

CHAPTER 3

MATERIALS AND EXPERIMENTS

3.1. Materials and compositions

Polycrystalline specimens of soft PZT (E_c~11 kV/cm) and hard PZT specimens were obtained from EDO Corp. (Salt Lake City, UT). In addition, PLZT 10/65/35 relaxor specimens were prepared, as previously reported. The specimens were cut into typical dimensions of 0.3 mm in thickness and 4 mm^2 in area, and were electroded with gold.

Single crystals of $Pb(Zn_{1/3}, Nb_{2/3})O_3$-4.5%$PbTiO_3$ (PZN-4.5%PT), and PZN-8%PT, grown by a top-seeded modified Bridgeman method, were obtained from TRS Ceramics (State College, PA). In addition, crystals of PMN-20%PT and PMN-30%PT were obtained from HC materials (Urbana, IL). Crystals of various orientations were studied, including $[001]_c$, $[110]_c$, and $[111]_c$. The specimens were also cut into typical dimensions of 0.3 mm in thickness and 4 mm^2 in area.

3.2. Polarization switching measurements

P-E measurements were made using a modified Sawyer-Tower bridge. This system was computer controlled and capable of automatic determination of standard P-E measurement compensation parameters. The system was capable of precise measurement of the P-E response over the frequency range of 10^{-3} to 10^2 Hz, the charge range of ~10 pC to 100 μC, and the current range of ~1 nA to 10 mA. A sinusoidal driving field was used.

The specimens were also studied using a current transient method. Investigations were performed for various fields of $0<E<3E_c$. In order to measure the response of the specimens over a broad time domain from $10^{-8}<t<10^2$ sec, three different measurements circuits were developed and built **[39].** Figure 3-1(a) shows the measurement circuit for

the short-time domain between 10^{-8} to 10^{-6} sec. Figure 3-1(b) shows the circuit for the middle-time domain between 10^{-6} to 10^{-3} sec. And, Figure 3-1(c) shows the circuit for the long-time domain between 10^{-3} to 10^{2} sec. For the short and middle time domains, the same procedure was used prior to switching. Initially the specimen was unpoled, and then an electric field of $-3E_c$ was applied to re-pole the specimen. To prepare for switching, both sides of the specimen were raised to the desired switching field. Then, at time t=0, one side of the specimen was taken to ground: this is an important step that allowed for the very highest current wall between the power amplifier and the specimen. By using these steps, we can certify that high voltage reaches its full maximum, before the polarization starts to rise. It was found that switching times of $<<10^{-8}$ seconds could be achieved. For the long-time domain, this method could also be used, but is not necessary as the rise time of the amplifier is significantly shorter than the measurement time. An Agilent oscilloscope operated in a time capture mode was used to measure the output voltage from each circuit. Figure 3-1 shows the circuits for short, middle and long time domains, respectively.

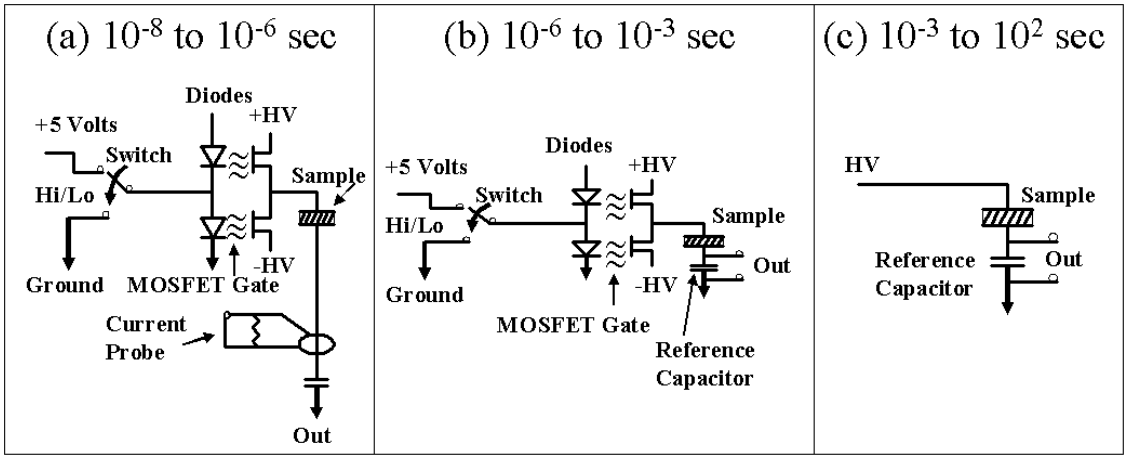

Figure 3-1. The three different measurements circuits. (a) short-time domain. (b) middle-time domain. (c) long-time domain.

CHAPTER 4

OBSERVATION OF BROAD RELAXATION TIME FOR POLARIZATION SWITCHING IN MODIFIED FERROELECTRICS

Investigations of the polarization dynamics over broad time and field regions would be greatly important to the study of modified ferroelectrics. It could significantly impact understanding of domain dynamics. In this chapter, we report the polarization dynamics over such a broad time domain, extending from $10^{-8}< t <10^{2}$ sec. We have studied various modified Pb-based ferroelectrics. Polycrystalline specimens of PMN-PT 70/30 (E_c~4 kV/cm) and PLZT 7/65/35 (E_c~6.7 kV/cm) were studied. Soft PZT (E_c~11 kV/cm) specimens obtained from EDO Corp. (Salt Lake City, UT), and a (001)-oriented single crystal of PMN-PT 70/30 obtained from HC Materials (Urbana, IL), were also studied. Studies were performed from E«E_c to E»E_c, where E_c is the coercive field. The results unambiguously demonstrate the presence of extremely broad relaxation time distributions for the switching process, extending over decade(s) in orders of magnitude in time, where the distribution is strongly dependent on E.

4.1. Polarization dynamics in soft ferroelectrics

Figure 4-1 shows the logarithm of the polarization as a function of the logarithm of time for (a) a PMN-PT 70/30 ceramic, (b) PLZT 7/65/35, (c) PZT, and (d) a (001)-oriented PZN-PT 4.5% crystal. All three of these specimens are soft ferroelectrics at room temperature, which have a modest E_c and relatively high susceptibilities. Data are shown for over ten decades in time, taken at various applied electric fields of 3<E<20 kV/cm. The data can be seen to be quite similar for all three compositions. It is similar for single crystals and polycrystals. Thus, the interesting general features of the data for the various compositions will be discussed together below.

(a) PLZT 7/65/35

(b) PMN30PT Ceramic

(c) Commercial soft PZT

(d) PZN4.5%PT $[001]_c$

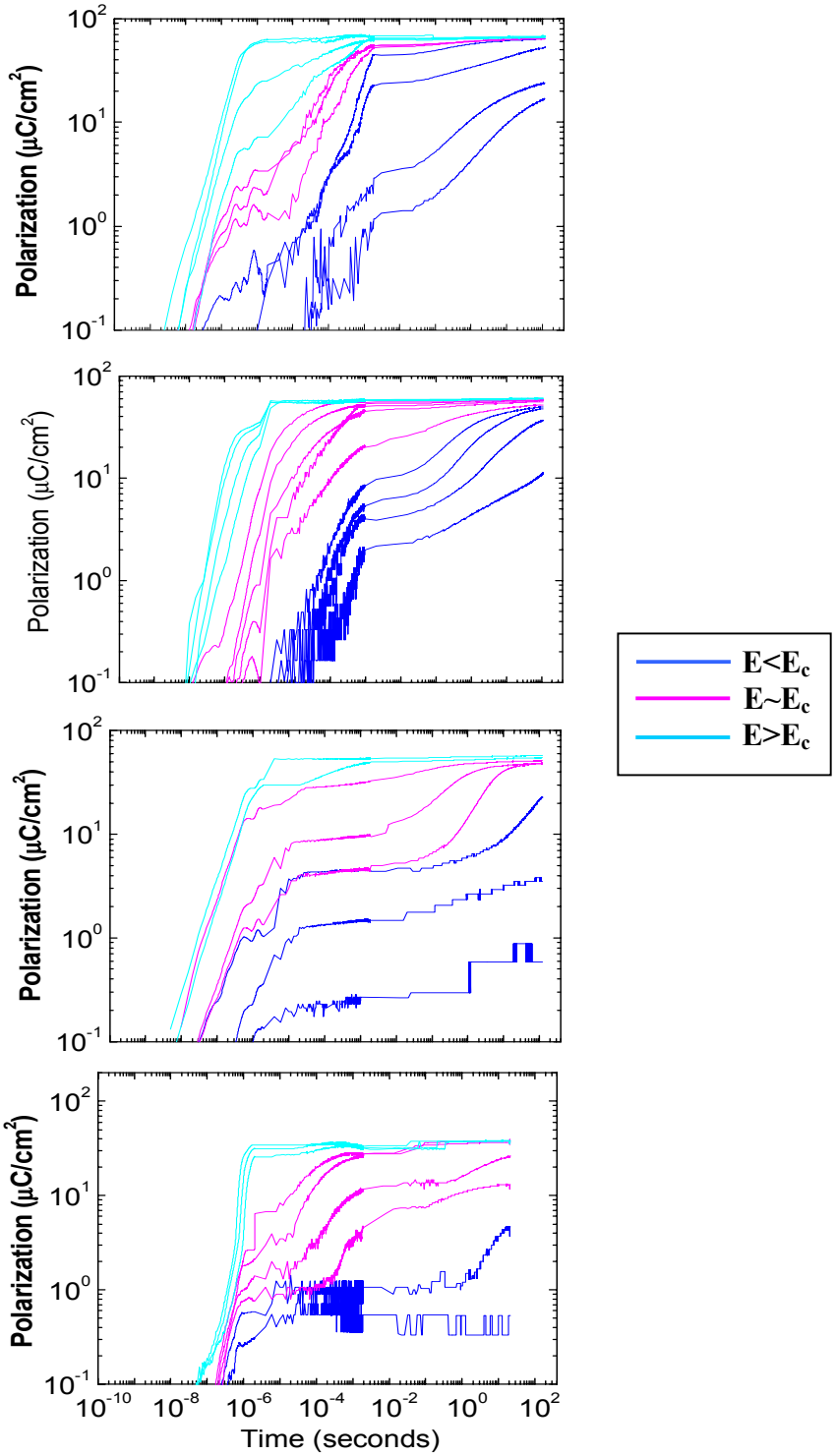

Figure 4-1. Logarithm of polarization as a function of logarithm of time for various "soft" ferroelectrics over broad time and field ranges. (a) PLZT 7/65/35, (b) PMN-30%PT, (c) a commercial "soft" PZT and (d) a (001) oriented PZN4.5%PT crystal. Data are shown for 3 different field regimes of $E<E_c$, $E\sim E_c$, and $E>E_c$ regimes.

The spectra can clearly be seen to be extremely broad in the time domain, extending over decade(s) of orders in magnitude. The spectra only became sharp at higher fields of $E \gg E_c$ and short times of $t<10^{-6}$ seconds. Unambiguously, polarization switching in soft ferroelectrics has a very broad distribution of relaxation times τ. It is important to note that the results for the PMN-PT ceramic where quite similar to those of the (001)-oriented crystal, demonstrating that the broadness in the time-domain is not due to a variety of extrinsic pinning sites such as grain boundaries and dislocations. The breadth of this distribution is nearly equal to that found in the weak-field susceptibility (dielectric constant) of relaxor ferroelectrics near their freezing temperature. However, there is structure within the spectra that changes with E and log(t). Below we use PLZT 7/65/35 as an example by which to discuss these features.

For $E<E_c$, as shown in Figure 4-2a, two regimes of different polarization responses were found. At short times of $10^{-5}<t<10^{-3}$ sec, the polarization logarithmically increased with t, exhibiting significant fluctuation (Barkhaussen-like) **[33]** events. With increasing E the randomness of the fluctuations decreased, and a plateau was found for $10^{-3}<t<10^{-1}$ sec. At longer times of $10^{-1}<t<10^{2}$ sec, the polarization smoothly and gradually increased with log(t). For $E<E_c$, polarization saturation seemingly would eventually be achieved, but only at times many orders of magnitude longer than 10^2 sec. For $E \approx E_c$, two regimes of polarization response were again present, as shown in Figure 4-2b. With increasing E, the regimes became increasingly indistinguishable in the time domain of $10^{-7}<t<10^{-3}$ sec. Complete saturation was only gradually approached for $t>10^{-3}$ sec. For $E>E_c$, the polarization response became increasingly sharp with increasing E, as shown in Figure 4-2c. For $E \gg E_c$, saturation was reached at $\sim 10^{-7}$sec.

We discuss our results in terms of a double well potential (Figure 4-3) that is under an applied electric field E and that has a rugged fine-structure, which is somewhat like that of a relaxor. For small E, Barkhaussen-like events occur as the system moves between rugged fine structures, towards the other variant – a polarization creep develops over long times. This creep occurs by stretched exponential functions **[22]**, due to the hierarchial nature of relaxation within a rugged landscape **[31-32].** With increasing E, the

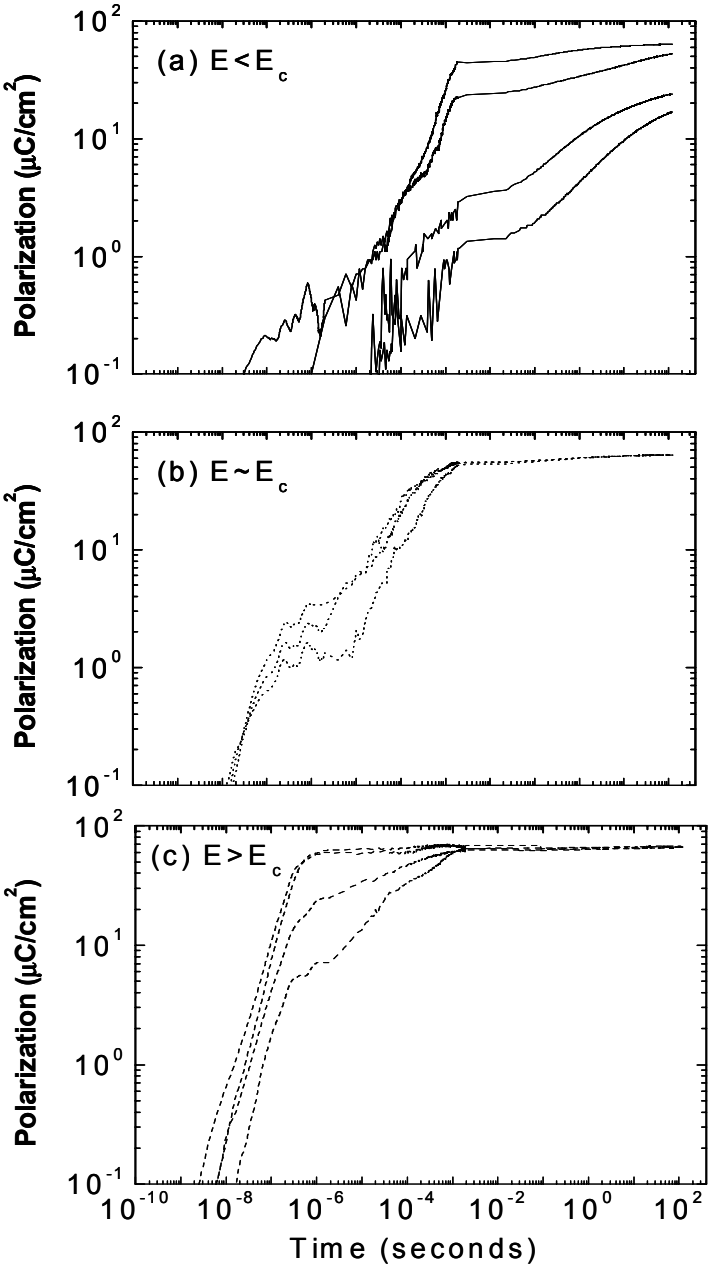

Figure 4-2. Logarithm of polarization as a function of logarithm of time for PLZT 7/65/35 for various field ranges. (a) $E<E_c$ [3, 4, 5, and 6kV/cm], (b) $E\sim E_c$ [6.4, 6.7, and 7kV/cm], and (c) $E>E_c$ [10, 15, 17, and 19kV/cm]. The fields shown in the brackets represent data from lower right to upper left in each figure.

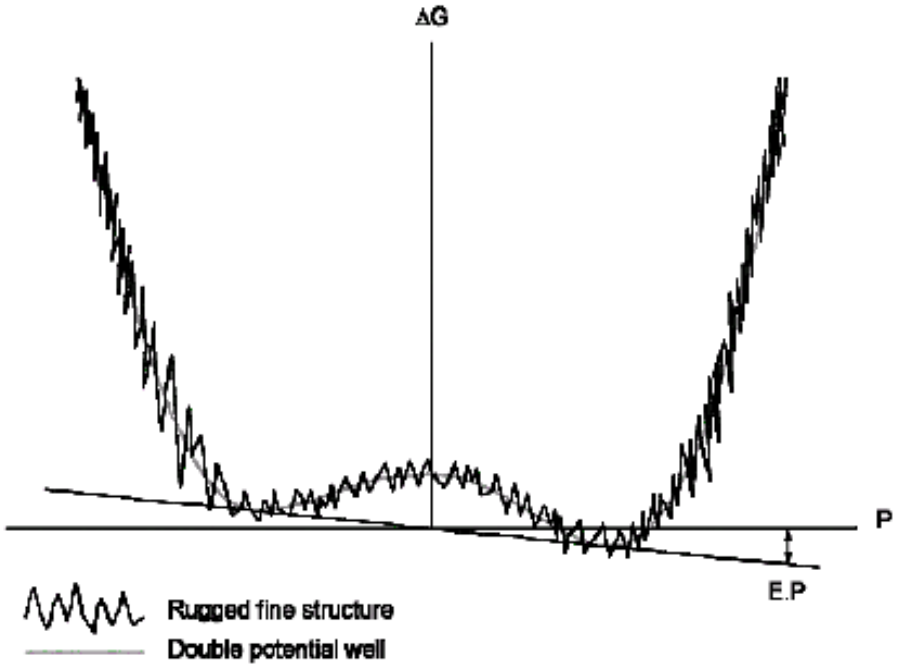

Figure 4-3. Illustration of double well potential with rugged fine-structure, which is under an applied electric field E.

system moves more freely within this landscape, and thus the breadth of the τ distribution and $\tau_{average}$ both decrease. At high fields of $E>>E_c$, polarization switching occurs rapidly and the τ distribution is sharp. In this field range, the dynamics can be described by an Avarami-type relationship, as the rugged landscape presents no impediments to switching.

Previous electron microscopy studies of soft ferroelectrics **[40]** have shown domain breakdown with increasing AC electric field. Furthermore, fractal domains have recently been used to understand long-time polarization dynamics in various modified PZTs. The results of our investigation demonstrate that soft ferroelectrics contain such heterogeneities under field for $E \leq E_c$, which control the dynamics of polarization switching. These heterogeneities are conceptually similar to the long-lived ones observed in relaxor ferroelectrics under weak field drive. At higher fields of $E>>E_c$, switching occurs by a mechanism similar to conventional ferroelectric domain nucleation and growth.

4.2. Summary

In summary, the polarization response of various modified soft Pb-based perovskites has been investigated over broad time and field ranges. The results unambiguously demonstrate the presence of extremely broad relaxation time distributions for switching in soft ferroelectrics, which can extend over decade(s) in orders of magnitude in time. With increasing field for $E>>E_c$, the breadth of the distribution is significantly sharpened, revealing that the switching mechanism is dependent on E.

CHAPTER 5

INVESTIGATION OF POLARIZATION SWITCHING IN ORIENTED $Pb(Zn_{1/3}Nb_{2/3})O_3$-4.5%$PbTiO_3$ CRYSTALS

Investigations of polarization dynamics of PMN-x%PT or PZN-x%PT for variously oriented crystals have not yet been performed. Such studies could provide important information concerning the mechanism of switching. In this investigation, we report the polarization dynamics over a broad time domain extending from $10^{-8}<t<10^{2}$ sec for $(001)_c$, $(110)_c$, and $(111)_c$ oriented PZN-4.5%PT crystals. Studies were performed from $E<<E_c$ to $E>>E_c$, where E_c is the coercive field. The results demonstrate the presence of extremely broad relaxation time distributions for the switching process, extending over decade(s) in orders of magnitude in time, where the distribution is strongly dependent on E.

5.1. Time Domain

Figure 5-1 shows the logarithm of the polarization as a function of the logarithm of time for PZN-4.5%PT crystals oriented along (a) the $(001)_c$; (b) the $(110)_c$; and (c) the $(111)_c$. Data are shown for over ten decades in time, taken at various applied electric fields. The spectra can clearly be seen to be extremely broad in the time domain, extending over decade(s) of orders in magnitude. The spectra sharpened at higher fields of $E»E_c$. Unambiguously, polarization switching for PZN-4.5%PT crystals has a very broad distribution of relaxation times τ. The breadth of this distribution is nearly equal to that found in the weak-field susceptibility (dielectric constant) of relaxor ferroelectrics near their freezing temperature **[41-43].** However, there were important differences between the spectra for the variously oriented crystals.

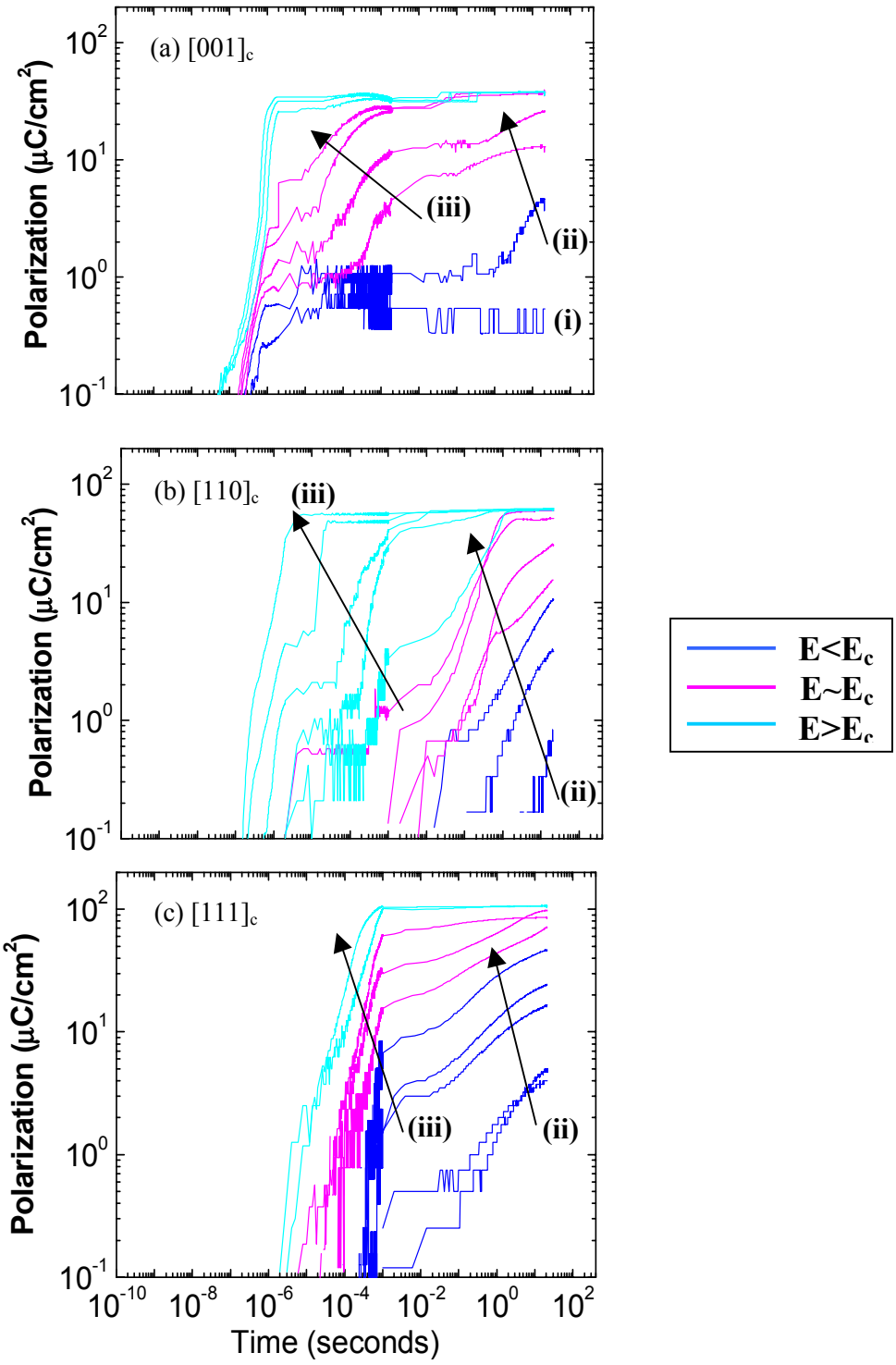

Figure 5-1. Logarithm of the polarization as a function of the logarithm of time for PZN4.5%PT crystals oriented along (a) the $[001]_c$, (b) the $[110]_c$, and (c) the $[111]_c$. Data are shown for over ten decades in time, taken at various applied electric fields.

5.1.1. Small fields applied along various orientations

At lower fields of E≈2 kV/cm applied along the $(001)_c$, a single transient was observed at $t \approx 10^{-6}$ sec, which was independent of time for $t > 10^{-5}$ sec. This transient is indicated by (i) in Figure 5-1(a). Whereas, along the $(110)_c$ and $(111)_c$, the time constant of the transient was dramatically longer near this field level – on the order of 1 to 10^2 sec. These transients are indicated by (ii) in Figures 5-1(b) and 5-1(c), respectively. The results clearly indicate an important difference between the variously oriented crystals. Along $(001)_c$, a rapid change in polarization occurs under a modest electrical field pulse, whereas such changes along $(110)_c$ and $(111)_c$ are dramatically slower.

5.1.2. Increasing E applied along $(001)_c$

For a field of E=3 kV/cm applied along $(001)_c$, a long-time polarization transient can be seen in the time domain of $1 < t < 10^2$ sec, as indicated in Figure 5-1(a) by the symbol (ii). With increasing field for 3<E<5 kV/cm, this long-time polarization transient was found to shift to shorter times. In addition, for 3<E<5 kV/cm, a third transient was observed in the intermediate time domain of $10^{-5} < t < 10^{-3}$ sec, as indicated in Figure 5-1(a) by the symbol (iii). This intermediate-time transient also shifted to shorter times with increasing E. For 3<E<5 kV/cm, the results show that a very rapid polarization response occurred at short times, followed by a delay, followed by an intermediate-time transient, followed by another delay, and finally followed by a long-time transient. With increasing E in this range, the three polarization processes can be seen to gradually merge at shorter times. For E>6 kV/cm, a single rapid – ballistic – polarization response was observed, whose time constant was $\sim 10^{-6}$ sec.

5.1.3. Increasing E applied along $(110)_c$ and $(111)_c$

Only two evolutionary stages in the time domain were found during polarization switching with increasing E applied along $(110)_c$ and $(111)_c$. At low fields, a long-time transient was found which shifted to shorter times with increasing E, as discussed in a

preceding subsection, and indicated by the symbol (ii) in Figures 5-1(b) and (c). For higher E, a second transient developed in the time domain of 10^{-4} sec, as indicated by the symbol (iii) in Figures 5-1(b) and (c). The results demonstrate a broad polarization transient in the intermediate time domain, followed by a delay, and a subsequent second broad polarization transient in the long-time domain.

It is important to note that long-time polarization transients were present to much lower fields along $(111)_c$, than along $(110)_c$. Clearly, there is an ease of the polarization response in the long-time domain along $(111)_c$ for fields of $E \ll E_c$. In fact, over the entire time-domain investigated, under the same applied field, the polarization response along $(111)_c$ was noticeable more rapid than that along $(110)_c$. At high fields, the two broad polarization transients can be seen to gradually merge, and a single more rapid polarization response to become evident.

In addition, along both $(111)_c$ and $(110)_c$, the leading edge of the polarization response at short times was noticeably field dependent, decreasing from $\sim 10^{-3}$ to $\sim 10^{-6}$ sec with increasing field between ~3 to ~12 kV/cm. Such a pronounced shift in the leading edge of the polarization response was not found along $(001)_c$, as its edge was always in the range of 10^{-6} sec.

5.2. Frequency Domain

Figure 5-2 shows a panel of P-E curves. The left column shows those along $(001)_c$, the middle column $(110)_c$, and the right one $(111)_c$. There are also three rows shown in the panel, which represent different maximum ac electric fields. The first row was for 2 kV/cm, the second 3 kV/cm, and the third 8 kV/cm. Each figure in the panel contains data taken at frequencies of 10^{-2}, 1, and 10^2 Hz.

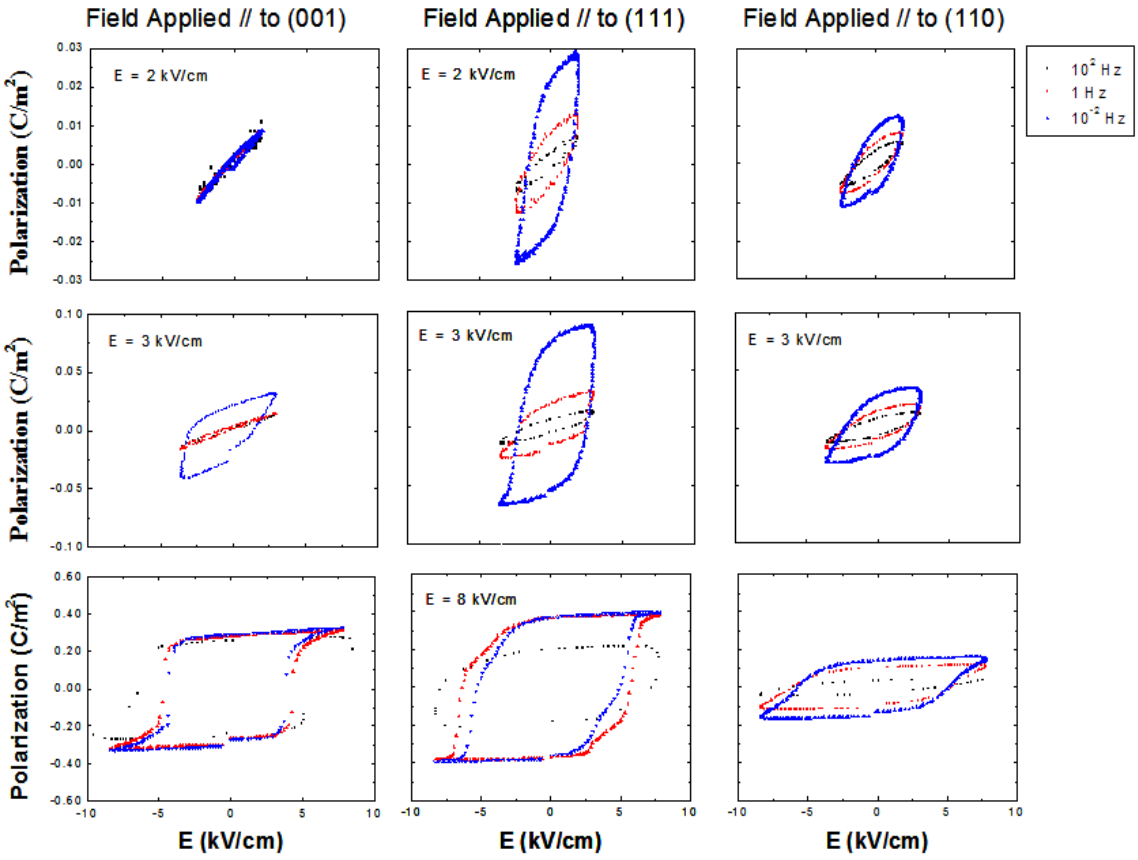

Figure 5-2. Panel of P-E curves. The three columns show those along $(001)_c$, $(111)_c$, and $(110)_c$, respectively.

5.2.1. Increasing E applied along $(001)_c$

For E≈2 kV/cm applied along $[001]_c$, a linear P-E response was found that was frequency independent. Also, the P-E response was anhysteretic. The induced polarization was ~0.01 C/m^2. The large amplitude dielectric constant can be calculated as

$$K = \frac{P}{\varepsilon_o E} = \frac{10^{-2} C/m^2}{8.85x10^{-12} F/m \;\; 10^5 V/m} \approx 5000;$$

where ε_o is the permittivity of free space. This large signal value of K was found to be equivalent to the weak field one measured using an Agilent 4284 LCR meter. This demonstrates that the P-E response along $(001)_c$ is a near ideal linear dielectric for E<2 kV/cm. Also, these results measured in the frequency domain are consistent with corresponding ones in the time domain, shown in Figure 5-1(a). The lack of time dependence for $t>10^{-5}$ sec is in agreement with the frequency independent response in the range of $10^{-2}<f<10^2$ Hz. The anhysteretic nature of the P-E response along $(001)_c$ demonstrates that the polarization mechanism is essentially non-dissipative for E<2 kV/cm.

Near ideal linear P-E behavior was observed along $(001)_c$ with increasing E to 3 kV/cm. However, nonlinearity and hysteresis began to be apparent, at low frequency. The onset of hysteresis corresponded to the appearance of a long-time polarization transient in the time domain data near $1<t<10^2$ sec, as illustrated in Figure 5-1(a) by the symbol (ii). As E was increased, significant hysteresis began to become apparent at increasingly lower frequencies. At higher fields, complete switching was observed in the P-E response. But, E_c was notably frequency dependent, shifting to higher values with increasing frequency, as previously reported for PMN-x%PT **[23]**. The results in the left hand panel of Figure 5-2 clearly show a transition with increasing field from a dynamical polarization process, which is non-dissipative and linear, to one, which is dissipative and nonlinear.

5.2.2. Increasing E applied along $(110)_c$ and $(111)_c$

However, for E≤2 kV/cm applied along either $(110)_c$ or $(111)_c$, a non-linear P-E response was found, which was strongly frequency dependent and hysteretic. Consider, for example a field of E=1 kV/cm applied along $(111)_c$, the induced polarization was ~0.03 C/m^2 at 10^{-2} Hz, which decreased to ~0.005 C/m^2 at 10^2 Hz. Correspondingly, the hysteretic losses decreased with increasing frequency. It is important to note that these frequency domain results are consistent with the corresponding time domain ones, which revealed long-time polarization transients in the time range of $10^{-2}<t<10^2$ sec for E=2 kV/cm. The pronounced hysteresis in the P-E response along $(111)_c$ and $(110)_c$ demonstrates that the long-time polarization transients are strongly dissipative. With increasing E to 3 kV/cm, the degree of polarization relaxation in the P-E response was found to increase. This increase corresponds to a shift to shorter times of the long-time polarization transient.

5.3. Fitting of Current Transients to Stretched Exponential Functions

The time-domain polarization data of Figure 5-1 were fit to equation (1.8), using a Levenberg-Marquadt nonlinear analysis. Multiple stretched exponential contributions were allowed for each data set. Two were sufficient to obtain good fitting to (1.8) along $(111)_c$ and $(110)_c$, whereas three were required along $(001)_c$. As discussed in paragraph 5.2, all three orientations had broad intermediate ($10^{-4}<t<10^{-2}$ sec) and long-time polarization transients (t>1 sec). In addition, along $(001)_c$, a third transient was found at short times of $t\approx10^{-6}$ sec.

The fitting of equation (1-7) to the data are shown in Figures 5-3, 5-4, and 5-5 for fields applied along $(001)_c$, $(111)_c$ and $(110)_c$, respectively. Four data sets are shown in each figure, to illustrate the changes in the time-domain polarization response with increasing E. The fitting to equation (1-7) is shown as a solid line in the plot, and the experimental data as small points. Inspection of this figure will reveal a very good fitting of the data to (1-7). This demonstrates that polarization switching in PZN-x%PT occurs by an extremely broad relaxation time distribution, typical of a stretched exponential

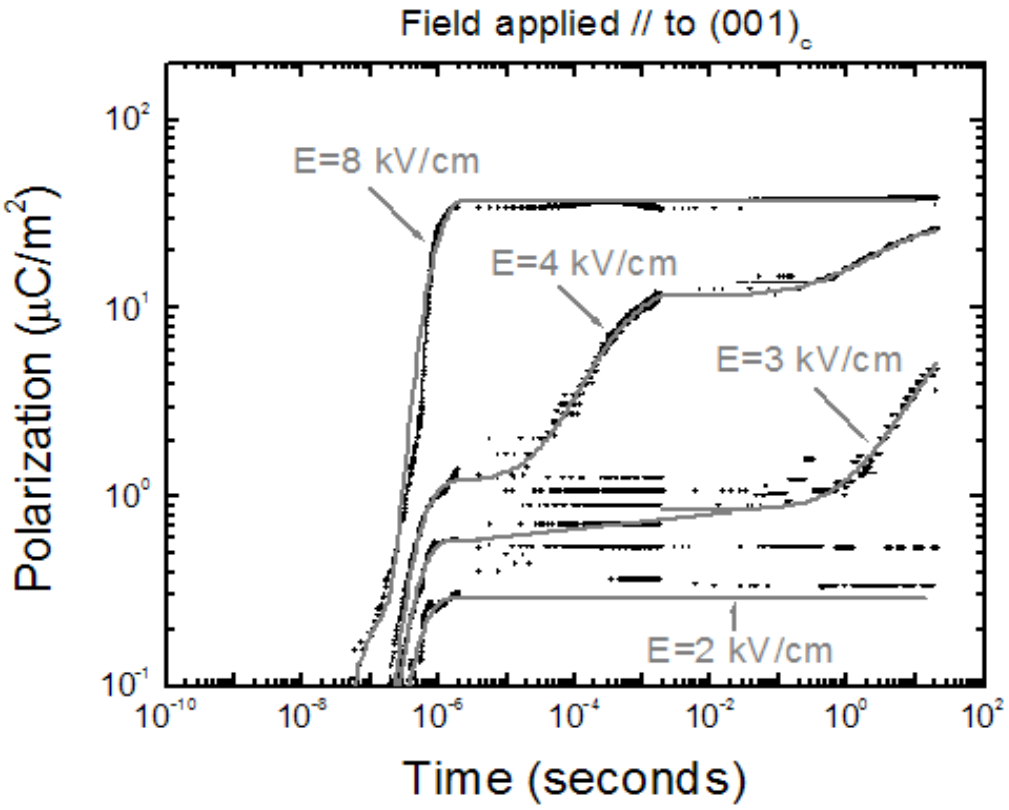

Figure 5-3. Fitting of equation (1.8) to the data for fields applied along $(001)_c$.

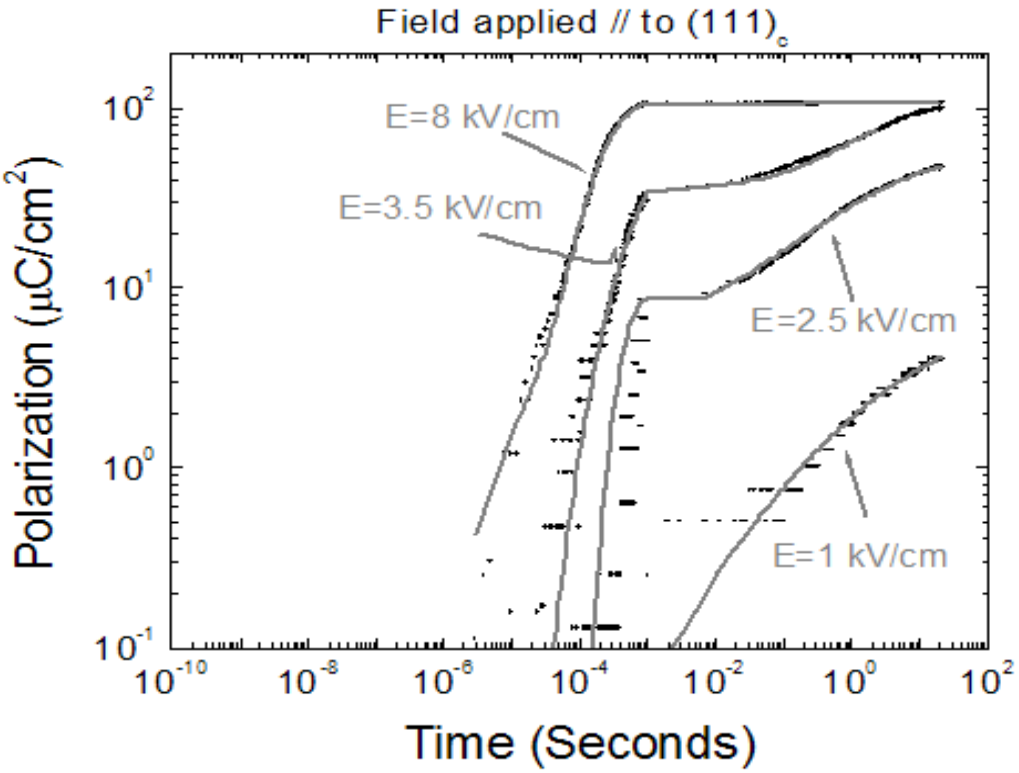

Figure 5-4. Fitting of equation (1.8) to the data for fields applied along $(111)_c$.

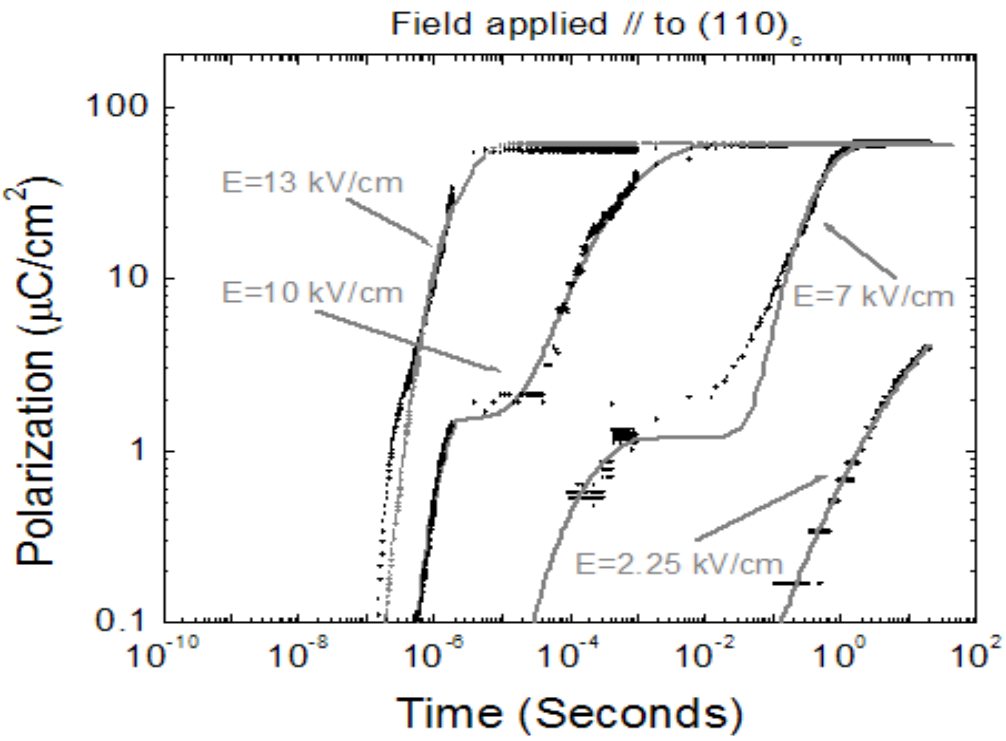

Figure 5-5. Fitting of equation (1.8) to the data for fields applied along $(110)_c$.

function (1.8); rather than a simple relaxation process with a well-defined singular relaxation time, typical of the Avarami equation (1.7b). High confidence levels were found in the fittings ($R^2 \approx 0.99$).

5.3.1. Dimensionality

The dimensionality factor, n, obtained from the fitting to (1.8) is shown in Figures 5-6(a)-(c) as a function of E along $(001)_c$, $(110)_c$ and $(111)_c$, respectively. It is important to note that n was always found to be very close to an integer value.

The rapid polarization response for $t<10^{-6}$ sec along $(001)_c$ was found to have $n \approx 3$, demonstrating that it is a volume process. The intermediate-time polarization transients along all three orientations were also found to have $n \approx 3$. Whereas, the long-time polarization transients observed along all three orientations were found to have $n \approx 2$, demonstrating that they are dimensionally confined to surfaces or boundaries.

5.3.2. Average relaxation times

The average relaxation time, τ, obtained from the fitting to (1.8) is shown in Figures 5-7(a)-(c) as a function of E^{-1} along $(001)_c$, $(110)_c$ and $(111)_c$, respectively. Along each direction there was more than one average relaxation time. This is because each data set required more than one stretched exponential function contribution. The value of τ is shown in each figure for every polarization transient in the respective specimens. The relaxation time τ was analyzed with a modified Arrhenius equation, given as;

$$\boldsymbol{\tau} = \boldsymbol{\tau}_o \exp[-E_o/E] \qquad (5.1)$$

where $\boldsymbol{\tau}_o$ is an attempt frequency of nucleation and E_o is an activation field.

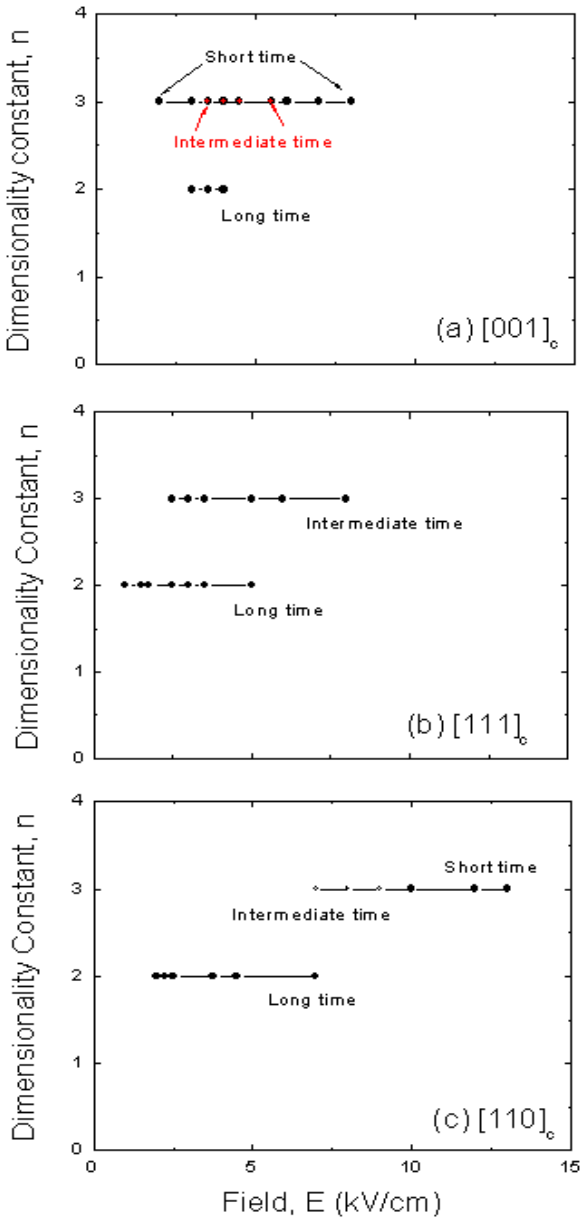

Figure 5-6. Dimensionality factor n obtained from the fitting to (1.8). (a) as a function of E along $(001)_c$, (b) $(111)_c$, and (c) $(110)_c$.

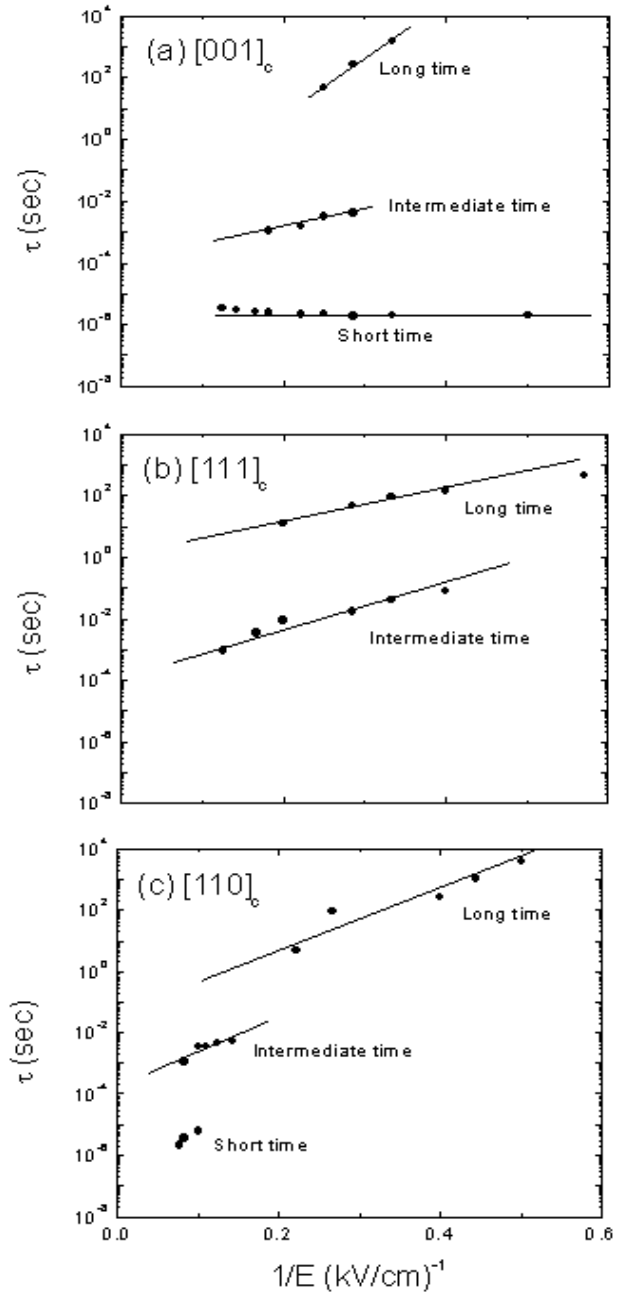

Figure 5-7. Average relaxation time τ, obtained from the fitting to (1.8). (a) as a function of 1/E along $(001)_c$, (b) $(111)_c$, and (c) $(110)_c$.

Along $(001)_c$, the rapid polarization response was found to have a value of $\tau \approx 10^{-6}$ sec, which was nearly unchanged with increasing E. This reflects the fact that the leading edge of the polarization response in the time domain was nearly independent of E over the range of fields investigated. Analysis with (5.1) yielded a value of $\tau_0 \approx 10^{-6}$ sec and an activation field of $E_o \approx 0$ kV/cm. The magnitude of the polarization switched by this rapid process varied significantly with E, however the kinetics of the response of this contribution were essentially unaltered.

Analysis with (5.1) was also performed on the long-time and intermediate-time polarization transients along all three orientations. The intermediate-time transients (i.e., nuclei formation) yielded close to the same value of $\tau_0 \approx 10^{-4}$ sec along all three directions. However, there was differences in the value of E_o, which was ~10 kV/cm along both $(001)_c$ and $(110)_c$, but was slightly less along $(111)_c$ with a value of $E_o \approx 6.5$ kV/cm. The long-time transients (i.e., domain growth) gave close to the same value of $\tau_0 \approx 10^{-2}$ sec along all three directions. Again, there was differences in the value of E_o, which was ~10 kV/cm along both $(001)_c$ and $(110)_c$, but was notably lower with $E_o \approx 2$ kV/cm along $(111)_c$. The significantly lower value of E_o along $(111)_c$ explains why there is an ease of the polarization response in the long-time domain for $E << E_c$.

5.4. Discussion and Summary

Evidence of nano-scale domain features in oriented PZN-4.5%PT has previously been reported – after switching under pulse fields – by atomic force microscopy (AFM) **[44].** Domain nuclei of nano-scale size were created under a reverse pulse of 3 kV/cm applied for 10^{-5} sec that were assembled into dendrite patterns, which were fractal in morphology, as shown in Figure 5-8(a). This is consistent with prior studies of soft ferroelectrics by Tan et al. **[38]**, who reported the breakdown of micron-sized ferroelectric domains into PNR with increasing E, and a high ac field induced relaxor state. Ex-situ AFM studies of switching **[44]** have also revealed with increasing pulse height to 10 kV/cm that the dendritic domains coarsened and that the density of nuclei is decreased, as shown in Figure 5-8(b).

Comparisons of our results with Figure 5-8 indicate that the polarization transient illustrated as (ii) in Figure 5-1 is due to creation of a high density of domain nuclei with a reversed polarization. Comparisons also reveals that the polarization transient illustrated as (iii) in Figure 5-1 is related to the assembly of the domain nuclei into ordered patterns or dendrites, which then grow into fully formed domain variants with reversed polarization. Both of these processes are extremely broad in the time domain.

5.4.1. Polarization rotation under small fields along $(001)_c$ $FE_{Ma} \rightarrow Fe_R$ transition

The rapid polarization response (n=3) along $(001)_c$ appears to be a nucleation process. However, it is unlike nucleation in that it is non-dissipative.

We can try to understand this by considering polarization rotation in the FE_{Ma} phase of PZN-4.5%PT. The polarization lies close to the $(111)_c$, but is slightly rotated towards $(001)_c$. Under applied field, polarization rotation gradually occurs with increasing E in the $(010)_c$ plane. It can rotate towards $(001)_c$ under forward field, or towards $(111)_c$ under reverse field. The nucleation barrier for polarization rotation is extremely small. Nuclei with a reversed polarization are not created. Thus, polarization response is essentially non-dissipative, and rapid.

5.4.2. Domain Nucleation and growth, with increasing E, along various orientations

With increasing pulse height applied along $(001)_c$, a secondary volume process (n=3) became obvious on longer time scales of $t>10^{-4}$ sec. A similar polarization transient in this time domain region was also found along $(110)_c$ and $(111)_c$.

This process appears to be the creation of domain nuclei with a reversed polarization. It is dissipative, as evidenced by hysteresis in the P-E curves. The fact that n=3 for this process indicates that nucleation is not confined to the vicinity of twin boundaries. Rather, it is a volume process; one that has a broad distribution of relaxation

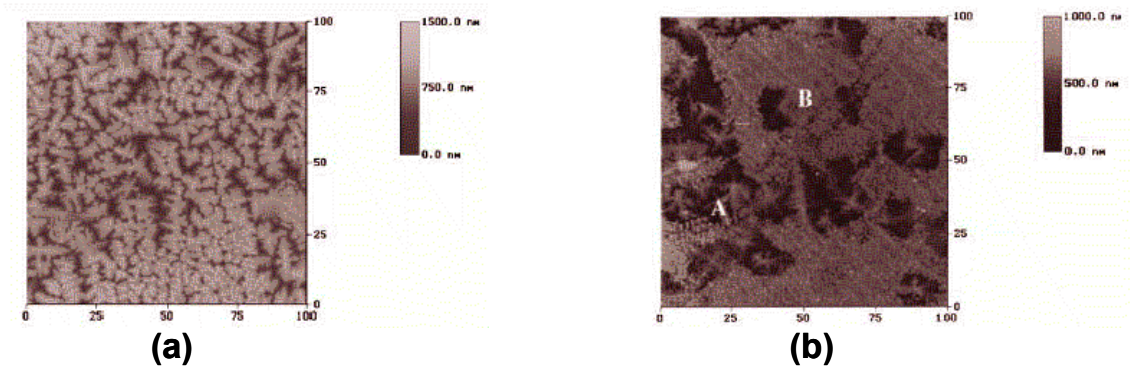

Figure 5-8. Dendrite domains patterns. (a) with a fractal morphology, (b) with a density of nuclei decreasing.

times, which is strongly suggestive of heterogeneous nucleation. At longer times of t>1 second, a boundary process (n=2) became evident. This process appears to be growth of the nuclei into fully formed domain variants with a reversed polarization. The broad distribution of relaxation times for this process indicates that the domain boundaries are fuzzy, or fractal in nature.

It should be noted that these two sequential steps (nucleation and growth) in polarization switching which were observed along all three orientations are separated by a hibernation period. With increasing field to $E>>E_c$, the two sequential (nucleation and growth) processes began (i) merging together; (ii) sharpening the relaxation time distribution; and (iii) shifting the average τ to noticeably shorter times.

Summary

The polarization response of variously oriented PZN-x%PT crystals has been investigated over broad time and field ranges. The results unambiguously demonstrate the presence of extremely broad relaxation time distributions for switching, which can extend over decade(s) in orders of magnitude in time. The polarization response over the time domain of $10^{-8}<t<10^{2}$ sec was well-fit to stretched exponential functions. Multiple stretched exponential contributions were required: one for domain nuclei formation, and a second for growth. Nuclei formation was found not to be restricted to domain walls, but rather was found to be a heterogeneous process. Direct observation of nano-sized domains or polar nuclei was provided by prior AFM imaging **[44].** The nucleation stage has heterogeneities similar to those of relaxor ferroelectrics. The growth stage has diffuse or fractal domain walls. At higher fields of $E>>E_c$, switching occurs by a ballistic mechanism.

CHAPTER 6

Comparisons of Polarization Switching in 'Hard', 'Soft', and Relaxor Ferroelectrics

Defects and substituents are known to significantly influence the electromechanical properties of ferroelectrics. Various classifications of piezoelectric behaviors have been categorized in lead zirconate titanate (PZT). The basic two types of classifications are commonly called 'soft' and 'hard'. In general, higher valent substituents induce soft piezoelectric behavior, where as lower valent ones induce hard. With increasing higher valent substituent concentration, a cross-over between soft and relaxor ferroelectric behavior occurs.

Soft ferroelectrics have lower coercive fields, higher hysteretic losses, higher dielectric and mechanical loss factors, and lower remanent polarizations and strains, relative to hard ones. The extra contribution is designated as extrinsic, and is believed to be due to domain dynamics under weak AC fields. Hard ferroelectrics have an asymmetric P-E response, which is shifted by a built-in potential. The built-in potential is due to a pinning of the polarization by dipolar defects. Relaxor ferroelectrics have a frequency dispersive dielectric response in the audio range; the inability to sustain remanence for temperatures above a freezing temperature T_f, which is notably less than that of the dielectric maximum (T_m); and by the presence of a local polarization until $T \gg T_m$.

Previous transmission electron microscopy (TEM) studies of soft, hard and relaxor ferroelectrics have shown dramatic differences in domain stability. Studies of hard ferroelectrics have shown fine "wavy" domains. Comparisons with dielectric property data indicated that the "wavy" domains result from pinning effects. Systematic studies of soft ferroelectrics have shown the development of increasingly irregular

domain morphologies with increasing higher valent substituent concentrations. And, above a critical concentration, polar nanodomains (PNR) form that have an average diameter between 30 and 50 Å, which is the relaxor state.

Domain dynamics are generally believed to make significant contributions to ferroelectric and piezoelectric properties. However, understanding them has proven difficult, in particular in systems containing significant concentrations of aliovalent substituents. Limiting the study of polarization switching and domain dynamics has been that current transient investigations have been performed over relatively narrow time (t) and electric field (E) ranges, even though the current response is known to be logarithmic in time. Nucleation and growth (N&G) models have previously been developed. However, analysis of the dynamics in the time domain of $10^{-8}<t<10^{-6}$ sec provides incomplete information, upon which to develop a comprehensive mechanistic understanding. Previous N&G models have been based on nucleation sites confined to existing domain walls (i.e., 2-D), with a subsequent restriction that during growth the domain walls remain coherent (i.e., 1-D). However, it is doubtful that such a model can explain switching in a wider range of aliovalently modified ferroelectrics.

Investigations of the polarization dynamics over broad time and field regions would be greatly important to the study of modified ferroelectrics. In this chapter, we report the polarization dynamics over such a broad time domain (extending from $10^{-8}< t <10^{2}$ sec) for hard, soft and relaxor ferroelectrics based on PZT. The results unambiguously demonstrate important differences in switching mechanisms between these general types of ferroelectrics.

6.1. Polarization switching analysis

Figure 6-1. shows the logarithm of the polarization as a function of the logarithm of time for (a) a soft PZT, (b) a relaxor PLZT 10/65/35, and (c) a hard PZT. These data were all taken at room temperature. Data are shown for over ten decades in time, taken at

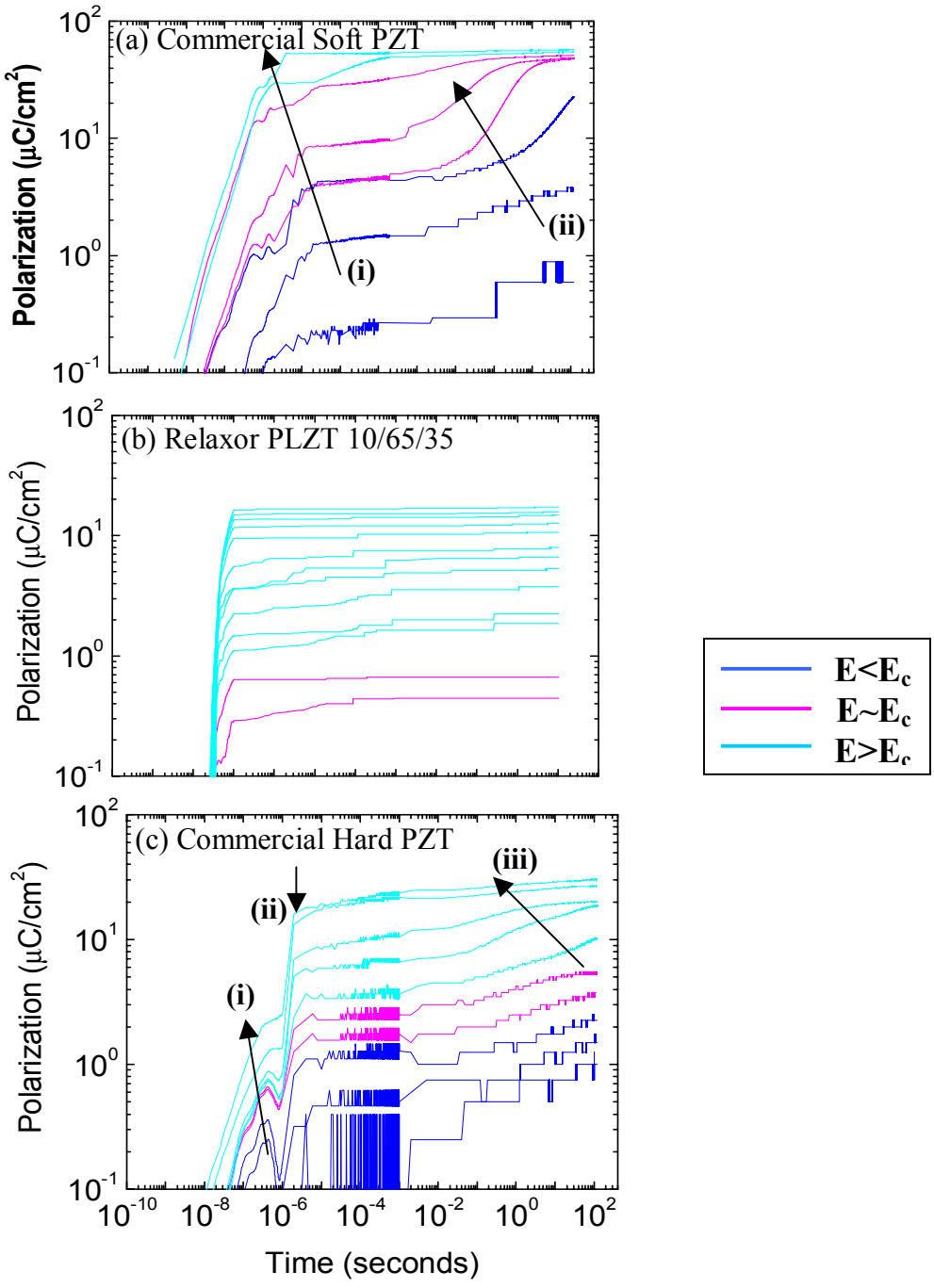

Figure 6-1. Logarithm of polarization as a function pf logarithm of time for various modified PZT ferroelectrics over broad time and field ranges: (a) soft PZT, (b) relaxor PLZT 10/65/35, and (c) hard PZT. Data are shown for various fields in each figure.

various applied electric fields. The data can be seen to be quite different for the three types of ferroelectrics.

6.1.1. Soft PZT

The response of soft PZT can clearly be seen to be extremely broad in the time domain, extending over decade(s) of orders in magnitude. Two evolutionary stages in the time domain were found during polarization switching with increasing E. Figure 6-1a demonstrates a broad polarization transient in the time domain of $10^{-6}<t<10^{-4}$ sec designated by the symbol (i) in the figure, followed by a delay, and a subsequent second broad polarization transient in the long-time domain designated by (ii). These two stages in the time domain response represent nucleation events and domain growth events, respectively. Recent investigations **[45]** of poled $Pb(Mg_{1/3}Nb_{2/3})O_3$-x%$PbTiO_3$ crystals have similarly shown two broad transients, demonstrating that the broadness in the time-domain is not due to a variety of extrinsic pinning sites such as grain boundaries and dislocations. With increasing E, both transients in Figure 6-1a shifted to shorter times, but only becoming sharp at high fields of $E»E_c$ and short times of $t<10^{-6}$ sec.

The time dependence of the polarization for soft PZT did not follow the Avarami (AV) equation, i.e., $P(t)=P_o \exp[-(t/\tau)^n]$ where τ is the relaxation time and n a dimensionality constant. Rather, as shown in Figure 6-2 (red line), it fit to a stretched exponential (SE) function, where terms in (t/τ) in the AV equation are replaced by ones in $\ln(t/\tau)$, i.e., $P(t)=P_o\exp[-a(\ln(t/\tau))^n]$. This demonstrates that the N&G events are extremely broadened in the time domain. Analysis with the SE equation yielded a value of n=3 for nucleation, and n=2 for growth. Nucleation is a 3-D process, and not confined to domain walls. Domain growth is a 2-D process, where the walls are not restricted to remain coherent. These results show that the domains walls are extremely diffuse during switching in soft PZT, and is consistent with prior TEM studies that have shown irregular domain morphologies.

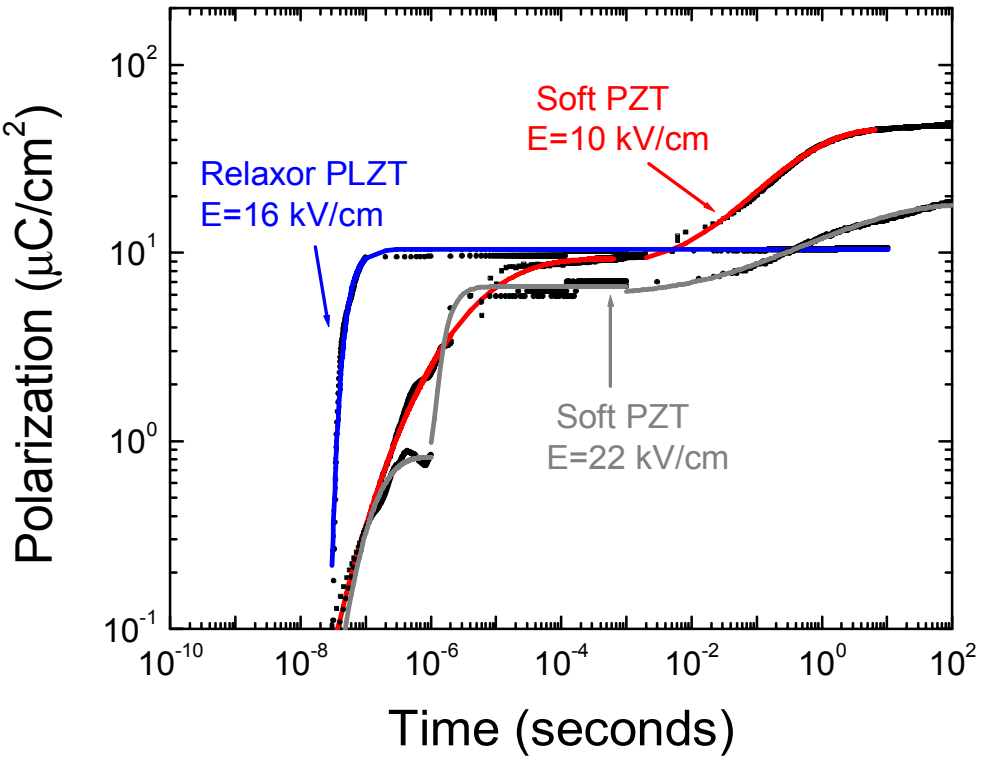

Figure 6-2. Illustration of fitting of time domain polarization response for soft, hard and relaxor ferroelectrics.

6.1.2. Relaxor PLZT 10/65/35

The relaxor PLZT 10/65/35 can be seen to have a very sharp response near $t=5x10^{-8}$ sec, as shown in Figure 6-1b. This sharp response did not shift in the time domain with increasing E, although the magnitude of the induced polarization did increase. The polarization only slightly increased with time for $t>10^{-7}$ sec. No secondary transient was found at longer times. It is relevant to note that at room temperature, PLZT 10/65/35 has slim loop P-E behavior and that $T>T_f$ (see Figure 6-3). The time dependence of the polarization for relaxor PLZT was found to be well fit to the AV equation, as shown in Figure 6-2 (blue line). Analysis yielded n=3 and $\tau=4.8x10^{-8}$ sec. No indication of a domain growth region was found. These results demonstrate that polarization reversal in the relaxors for $T>T_f$ occurs entirely by nucleation. The results are consistent with prior TEM studies that have shown pre-existing polar nuclei or PNR **[46-47]** under zero field.

6.1.3. Hard PZT

Hard PZT was found to have three evolutionary stages. Figure 6-1c shows a broad polarization transient in the time domain of $10^{-8}<t<10^{-6}$ sec designated as (i) in the figure. This transient was similar to that observed in soft PZT. Analysis with the SE equation yielded a value of n=3, as shown in green in Figure 6-2. Then, at $t\approx10^{-6}$ sec, a sharp increase in P was found, which is designated as (ii). The sharpness of this peak is similar to that observed for the relaxor, but $\tau=10^{-6}$ sec, rather than 10^{-8} sec. This portion of the time domain response was found to be well fit by the AV equation with n=3, and its position in the time domain did not shift with increasing E. Finally, a weak long-time polarization transient for t>1 sec was found at higher E, designated by (iii). It is analogous to that in soft PZT, but was much weaker and was only noticeable at much higher E. This long-time transient was well fit by the SE equation with n=2, again in analogy with soft PZT.

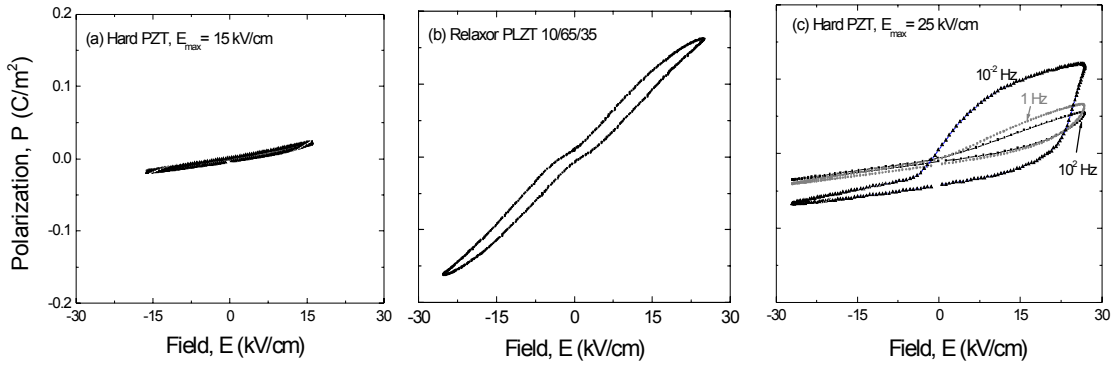

Figure 6-3. P-E response for (a) hard PZT with E=15 kV/cm, (b) relaxor PLZT 10/65/35 with E=25 kV/cm and (c) hard PZT with E= 25kV/cm. Please notice the anhysteretic nature of (a) and (b), whereas (c) exhibits dramatically increased hysteresis with decreasing measurement frequency.

The results for hard PZT demonstrate that the switched polarization is mainly due to nucleation. The data show a switchover from SE type nucleation events to AV ones. It is important to note that the fraction of polarization switched by nucleation is much higher for hard PZT, than soft. This is because domain growth is not significant for hard PZT. The switchover to AV type nucleation near $t=10^{-6}$ sec may reflect a transition to a state with a high density of stable polar nuclei or PNR, somewhat similar to the relaxor, which then do not grow readily into fully formed domain variants with a reversed polarization due to built-in dipolar fields.

6.2. P-E measurements

We also found that nucleation is only slightly dissipative, whereas domain growth is strongly so. This is illustrated in the P-E curves given in Figures 6-3 for (a) hard PZT with E=15 kV/cm, (b) relaxor PLZT, and (c) hard PZT with E=25 kV/cm. The P-E response for both (a) and (b) were nearly anhysteretic and nondispersive over the frequency range of $10^{-2}<f<10^{2}$ Hz. Clearly, nucleation is not significantly dissipative. However, for hard PZT with E=25 kV/cm, hysteresis became evident with decreasing f, as shown in (c). The onset of hysteresis corresponds to the development of a long-time polarization transient in the time domain data with increasing E. These results indicate that nucleation events occur against a small anisotropy barrier. In this regard, nucleation events may be similar to polarization rotation in poled PMN-PT crystals, with gradual structural evolution. However, in our case, rotation clearly must be an inhomogeneous process.

6.3. Summary

In summary, the polarization response of hard, soft, and relaxor ferroelectrics have been investigated over broad time and field ranges. The results unambiguously demonstrate important differences in the polarization switching mechanism between these families of materials.

In soft PZT, there are two stages in the time domain response corresponding to the nucleation and growth events. Those two events are extremely broadened in the time domain. The broadness in the time-domain is not due to a variety of extrinsic pinning sites such as grain boundaries and dislocations. In relaxor PLZT 10/65/35, there is only one sharp transient near $t=5x10^{-8}$ sec corresponding to a very fast nucleation. There is no indication of a domain growth region. Polarization switching only occurs by nucleation. Hard PZT has three evolutionary stages. The fraction of polarization switched by nucleation is much higher for hard PZT, than soft. This is the reason why domain growth is not significant for hard PZT, rather than nucleation of polar nuclei, which then do not grow readily into fully formed domains.

CHAPTER 7

CONCLUSIONS

In Chapter 4, polarization reversal over extremely broad time domain and field ranges in various soft ferroelectrics has been investigated. The results demonstrate the presence of extremely broad relaxation time distributions for switching, which can extend from $10^{-8} < t < 10^{2}$ sec. At relatively small fields of $E \ll E_c$, the relaxation time distribution is very broad and depends on E; whereas at higher fields of $E \gg E_c$, the breath of the distribution is significantly sharpened.

In Chapter 5 was studied polarization switching over broad time domain and field ranges for $[001]_c$, $[110]_c$, and $[111]_c$ oriented PZN-4.5%PT crystals. The transients over the time domain of $10^{-8} < t < 10^{2}$ sec were well-fit to stretched exponential functions. These results demonstrate that the nucleation stage is a volume process, which has heterogeneities similar to the long-lived ones observed in relaxor ferroelectrics. Domain growth was also found to be broad in the time domain, indicating diffuse or rough domain walls. At higher fields of $E \gg E_c$, the relaxation time distribution becomes very sharp. This indicates that polarization switching occurs by a mechanism similar to conventional domain nucleation and growth.

Chapter 6 presents a comparative study of polarization switching in "hard", "soft", and "relaxor" Pb-based polycrystalline ferroelectrics. The results unambiguously demonstrate important differences in the current transients and relaxation time distribution. Evidence of differences in the polarization switching mechanism is given for these various types of ferroelectrics. It was shown that domain growth is not significant for "hard" PZT, whereas "soft" PZT exhibits extremely broad nucleation and growth events. And, in relaxor ferroelectrics, polarization reversal occurs entirely by nucleation.

BIBLIOGRAPHY

Abplanalp M., D.Barosova, P.Bridenbaugh, J.Appl.Phys., vol.91, p.3797 (2002) **[12]**

Bellaiche L., A. Garcia, and D. Vanderbilt, Phys. Rev. Lett. 84, 5427 (2000) **[9]**

Benedetto J.M., R.A. Moore, and F.B. McLean, J. Appl. Phys. 75, 460 (1994) **[24]**

Boscolo I. and S. Cialdi, J. Appl. Phys. 91, 6125 (2002) **[21]**

Chen J., H. Chan and M. Harmer, J. Am. Ceram. Soc. 72, 593 (1989) **[36]**

Cross L.E., Ferroelectrics 151, 305-315 (1994) **[35]**

Dai X.H., Z.Xu, and D.Viehland, Phil. Mag. B70, 33-48 (1994) **[46]**

Dalton J., Phys. Rev. 133A, 1034 (1964) **[25]**

Drougard M.E., J. Appl. Phys. 31, 352-355 (1960) **[14]**

Fu H. and R. Cohen, Nature 403, 281 (2000) **[8]**

Hutton S., U. Hochli, M. Magilone, ed. I. Campbell and C. Biovannella, (Plenum, NY), 289 (1990) **[32]**

Imry Y. and S. Ma, Phys. Rev. Lett. 35, 1399-1402 (1975) **[28]**

Ishibashi Y., and Y. Takagi, J. Phys. Soc. Japan 31, 506-511 (1971) **[17]**
Ishibashi Y., Integrated Ferroelectrics 2, 41 (1992) **[19]**

Jullian C., J.F.Li, D.Viehland, Appl. Phys. Lett. 83 (11 Aout 2003) **[45]**

Kleeman W., Intern. J. Mod. Physics 7, 2469 (1993) **[33]**

Kuwata J., K.Uchino and S.Nomura, Jpn. J. Appl. Phys., 21, 1298 (1982) **[2]**

Levstik A., M. Kosec, V. Bobnar, C. Filipic, and J. Holc, Jap. J. Appl. Phys. 36, Pt. 1, No. 5A, 2744-2746 (1997) **[18]**

Merz W.J., Physical Review, 95, 690-698 (1954) **[13]**

Miller R.C., and G. Weinreich, Phys. Rev. 117, 1460-1466 (1960) **[15]**

Mydosh J., Taylor and Francis, London (1993) **[31]**

Nattermann T. and J. Villain, Phase Transitions 11, 5-20 (1988) **[29]**

Noheda B., J.A.Gonzalo, L.E.Cross, R.Guo, S.E.Park, D.E.Cox, and G.Shirane, Phys. Rev. B61, 8687, (2000) **[3]**
Noheda B., J.A.Gonzalo, L.E.Cross, D.E.Cox, and G.Shirane, Appl. Phys. Lett. 74, 2059, (1999) **[4]**
Noheda B., L.E.Cross, D.E.Cox, G.Shirane, S.E.Park and Z.Zhong, Phys. Rev. Lett. 86, 3891, (2001) **[5]**

Ohwada K., K.Hirota, P Rehrig, Y. Fujii, and G. Shirane, Phys, Rev B arXIV: Cond-mat/0207726 v3, (12 Aug 2002) **[6]**

Randall C., D.Barber, and R.whatmore, J. Mocrosc. 45, 275 (1987) **[47]**

Scott J.F., L. Kammerdiner, M. Parris, S. Traynor, V. Ottenbacher, A. Shawabkeh, and W. Oliver, J. Appl. Phys. 64, 787 (1988) **[26]**
Scott J.F., Springer, Berlin (2000) **[27]**

Shur V., E. Rumyantsev, and S. Makarov, J. Appl. Phys. 84, 445-451 (1998) **[16]**

Smolenskii G.A. and A. Agranovskaya, Sov. Phys. Sol. State 1, 1429-1441 (1960) **[34]**

Song T., S. Aggarwal, Y. Gallais, B. Nagaraj, R. Ramesh, and J. Evans, Appl. Phys. Lett. 73, 3366-3368 (1998) **[20]**

Tan Q. and Dwight Viehland, Phys. Rev. B 53, 14103-14111 (1996) **[38]**
Tan Q., PhD Dissertation, University of Illinois, Urbana, IL (1998) **[40]**

Viehland D., M. Wuttig, and L.E. Cross, J. App. Phys. 68, 2916-2924 (1991) **[41]**
Viehland D., M. Wuttig, and L.E. Cross, Phil. Mag. B 64, 335-344 (1991) **[42]**
Viehland D., M. Wuttig, and L.E. Cross, Ferroelectrics 120, 71-77 (1991) **[43]**
Viehland D., N. Kim, Z. Xu, and D. Payne, J. Am. Cer. Soc. 78, 2481-2489 (1995) **[37]**
Viehland D., JF.Li and Q.Tan, Philo.Magazine B, vol.76, 59-74, (1997) **[1]**
Viehland D., and Y.Chen, J. Appl. Phys., 88, 6696, (2000) **[23]**
Viehland D., J. Appl. Phys. 88, 4794-4806 (2000) **[10]**
Viehland D., and J.Power, J. Appl. Phys., vol.89, p. 1820 (2001) **[11]**
Viehland D., and J.F. Li, J. Appl. Phys. 90, 2995 (2001) **[22]**
Viehland D., J.F.Li, Appl. Phys. 92, 7690 (2002) **[7]**

Villian J., J. Physique 46, 1843-1852 (1985) **[30]**

Yu H., V. Gopalan, J. Sindel, and C. Randall, J. Appl. Phys. 89, 561 (2001) **[44]**

We acknowledge that the control units and high-voltage test heads were designed and built by Paul Moses, State College, PA 16801 **[39]**

VITA

Christelle Jullian was born in Montpellier, France, on July 27, 1979. She graduated from the University of Technology of Compiegne, France, in 2002 with a Bachelor of Mechanical Engineering.

She worked as a visiting scholar in the University of Virginia Polytechnic Institute beginning in January 2002. She has authored 1 paper and 2 letters. She is a member of the American Ceramic Society.